Notes on Nonlinear Dynamics, CMI, Spring 2020

Govind S. Krishnaswami, 22 April, 2020

Please let me know at govind@cmi.ac.in of any comments or corrections

Contents

1 Introductory remarks on dynamical systems

We will be concerned with time evolution (or dynamics) of systems with finitely many degrees of freedom. A typical example is a mechanical systems of finitely many (N) particles, that is described by ordinary differential equations (ODEs), say for the positions $\mathbf{r}_1(t), \cdots, \mathbf{r}_N(t)$ of the particles, with only one independent variable (time). This is in contrast to *fields* (such as velocity $\mathbf{v}(\mathbf{x}, t)$ and density $\rho(\mathbf{x}, t)$) that occur, say, in fluid mechanics or gravity or electromagnetism and are modeled by partial differential equations (PDEs) with more than one independent variable ($\mathbf{x}$ and t). There are two main types of dynamical systems we will consider: continuous time and discrete time. The former are modeled using (systems of first order) ordinary differential equations (ODEs), e.g., the three equations

$$\frac{d\mathbf{x}}{dt} = \mathbf{v}(\mathbf{x}, t) \quad \text{for} \quad t \geq 0, \quad \text{with} \quad \mathbf{x}, \mathbf{v} \in \mathbb{R}^3 \quad \text{and initial condition} \qquad \mathbf{x}(0) = \mathbf{x}_0 \tag{1}$$

This 'initial value problem' (IVP) is, in general, a nonlinear system of equations, as the vector field $\mathbf{v}$ need not be a linear function of $\mathbf{x}$. Time is the only independent variable. The space in which the dependent variables $\mathbf{x}$ take values ($\mathbb{R}^3$ here) is called the state space or phase space. The number of dependent variables is the dimension of the phase space. The curve $\mathbf{x}(t)$ parametrized by time is called the phase trajectory or the integral curve of the vector field. The system is called autonomous if $\mathbf{v}$ does not depend explicitly on time. We can think of $\mathbf{v}$ as the prescribed[1] velocity field in a fluid flow and of $\mathbf{x}$ as the position of a test particle that is carried around by the flow. The system is autonomous if the fluid flow is steady. We note that a higher order ODE can be reduced to a system of 1st order ODEs by introducing additional dependent variables. E.g., Newton's equation for the pendulum's angle of deflection from the vertical, $m\ddot{\theta} = -(g/l)\sin\theta$ becomes the pair of autonomous nonlinear first order ODEs by introducing $p = ml^2\dot{\theta}$ as a new variable

$$\begin{pmatrix} \dot{\theta} \\ \dot{p} \end{pmatrix} = \begin{pmatrix} p/ml^2 \\ -gl\sin\theta \end{pmatrix} \tag{2}$$

They become linear in the simple harmonic approximation $\sin\theta \approx \theta$. A non-autonomous system of n ODES $\dot{x}^i = v^i(\mathbf{x}, t)$ can be turned into an autonomous one by introducing an extra dependent variable $x^{n+1} = t$, so that

$$\begin{pmatrix} (\dot{x}^i)_{1\leq i\leq n} \\ \dot{x}^{n+1} \end{pmatrix} = \begin{pmatrix} (v^i(\mathbf{x}, x^{n+1}))_{1\leq i\leq n} \\ 1 \end{pmatrix}. \tag{3}$$

In other words, a time-dependent vector field on $\mathbb{R}^n$ may be viewed as a time-independent vector field on $\mathbb{R}^{n+1}$.

Discrete time dynamical systems are modeled by (systems of) difference equations. The primary examples are iterated maps of a real or complex variable, such as

$$z_{n+1} = f(z_n) \quad \text{for} \quad n = 0, 1, 2, \cdots, \quad \text{where} \quad f(z) = z^2 + i \quad \text{with} \quad z_0 = 1. \tag{4}$$

$n = 0, 1, 2, \ldots$ plays the role of a discrete time variable and the sequence z_n is the analogue of the phase trajectory. Maps sometimes arise by observing a continuous time system at certain discrete instants of time, just as the ODEs for some dynamical systems (e.g. the Lorenz

[1] $\mathbf{v}(\mathbf{r}, t)$ is given. It is not dynamical in the sense that we are not given an evolution equation for $\mathbf{v}$.

model) arise as simplifications/reductions of PDEs describing evolving fields (e.g. atmospheric convection). Indeed, Poincaré proposed to obtain information about solutions to a system of ODEs by examining the points where a trajectory intersects a fixed Poincaré surface in phase space. A trajectory beginning at $t = t_0$ at a point x_0 on the surface [and that is transversal (goes off it) to the surface] may first return to a point x_1 on the surface at a later time t_1. The map $x_0 \mapsto x_1$ is called the Poincaré first return map and it defines a discrete time dynamical system. Iterating the return map, we record all locations at which the trajectory intersects the surface to obtain its Poincaré section. For instance, the Poincaré section of a periodic trajectory consists of a finite number of points (among which the discrete dynamics periodically circulates). Discrete time dynamical systems also arise via finite difference approximations that are used in numerical schemes to solve ODEs. For instance, the ODE $\dot{x} = v(x)$ may be discretized as

$$x(t + \delta t) - x(t) \approx \delta t \, v(x(t)) \quad \text{for small } \delta t \tag{5}$$

Denoting $x(t) = x_n$ and $x(t + \delta t) = x_{n+1}$ we define the map

$$x_{n+1} = x_n + \delta t \, v(x_n) \equiv f(x_n) \tag{6}$$

whose successive iterates (for sufficiently small δt) can provide an approximation to the phase trajectory. The first-order nature of the underlying ODE ensures that (at least in this 'forward Euler' scheme) x_{n+1} depends only on x_n (and not, say, x_{n-1}).

• See S H Strogatz, *Nonlinear Dynamics and Chaos* for a good introduction to this subject.

2 Flows in 1D: Vector field on the real line

We begin by considering the autonomous first order ODE $\dot{x} = v(x)$ where the dynamical variable x is real and subject to the initial condition $x(0) = x_0$. Here v may be viewed as the velocity field of a fluid flowing steadily on the line and $x(t)$ the trajectory of a test particle that is released into the flow at x_0. Such an equation can be reduced to quadrature (evaluation of integrals)

$$\int_0^t dt' = t = \int_{x_0}^{x} \frac{dx'}{v(x')}. \tag{7}$$

In favorable cases, the integral can be evaluated in closed form to give t as a function of x. We would still have to invert the result to express x as a function of time. This is not always easy to do, as the example $v(x) = -\sin x$ reveals

$$-t = \log \frac{|\csc x_0 + \cot x_0|}{|\csc x + \cot x|}. \tag{8}$$

The example $\dot{x} = -\sin x$, which we will further examine below, arises in an overdamped limit of a pendulum. A pendulum subject to damping may be modeled by the second order Newtonian ODE $ml^2\ddot{\theta} = -\gamma\dot{\theta} - mgl\sin\theta$. $\gamma > 0$ is the damping coefficient. In the overdamped limit, we ignore the inertia/acceleration term altogether to arrive at $\dot{\theta} = -(mgl/\gamma)\sin\theta$. In this limit, Newton's equation changes character, it goes from being second-order to first order[2].

Aside from their intrinsic interest and as a simple starting point for the study of dynamical systems, flows in 1d can also capture some essential features of flows in higher dimensions. For

[2]The inertia term is said to be a singular perturbation of the overdamped equation.

instance, due to dissipation, higher dimensional flows can sometimes undergo a 'dimensional reduction' and behave in effect like 1d flows.

2.1 Fixed points, phase portrait, linear stability

Fixed points and phase portrait: Even without an explicit expression for $x(t)$, much qualitative insight may be gained by studying the geometric nature of $v(x)$, as emphasized by Poincaré. If x_* is a zero of $v(x)$, then it is a 'stagnation' point, where the fluid is at rest. So we have a static/equilibrium/constant solution $x(t) \equiv x_*$ for all t at each zero (or 'fixed point') of v. On the other hand, if $v(x) \neq 0$, then the particle moves to the right/left at x depending on whether $v(x)$ is positive or negative. Moreover, if $|v(x)|$ is increasing, then the particle speeds up while it decelerates if $|v(x)|$ is decreasing. These observations are enough to get a qualitative understanding of trajectories. They are usefully displayed on a phase portrait, which is a diagram of the phase space showing the qualitatively different trajectories.

• For instance, for $v(x) = -\sin x$, the fixed points are at $x = 0, \pm\pi, \pm 2\pi, \ldots$. The flow is to the left for $2n\pi < x < (2n+1)\pi$ and to the right on $((2n-1)\pi, 2n\pi)$ for any integer n. This may be displayed on a phase portrait, which in this case, is the real line with fixed points at integer multiples of π and the direction of trajectories between successive fixed points indicated by arrows. Draw the phase portrait and also roughly plot some trajectories on the $t - x$ plane. Non-constant trajectories monotonically approach a fixed point as $t \to \infty$ and emerge from a neighboring fixed point as $t \to -\infty$. We will see why it takes infinitely long. In particular, the trajectories do not display any oscillations.

• The fixed points may be classified by their stability. In the above example, odd multiples of π are unstable as the flow is directed away from them in both directions. On the other hand, even multiples of π are stable fixed points.

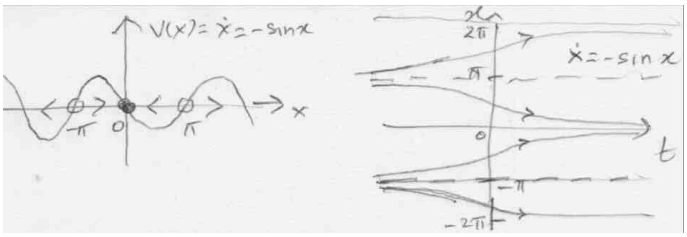

Figure 1: Phase portrait and trajectories for $\dot{x} = -\sin x$.

• A third possibility is provided by the fixed point at the origin for the vector field $v(x) = x^2$. In this case, the flow is directed rightward at all $x \neq 0$. So $x = 0$ is 'half-stable': stable on the left but unstable on the right. Notice that trajectories either go off to ∞ or approach the fixed point $x = 0$ in a monotonic fashion.

Linear stability: The stability/instability of a fixed point may be quantified by a decay/growth rate that controls how fast the phase point approaches/leaves the fixed point from its immediate vicinity. It is obtained by linearizing the vector field in the neighborhood of the fixed point x_*:

$$\dot{x} = v(x) = v(x_*) + v'(x_*)(x - x_*) + \ldots \approx v'(x_*)(x - x_*), \tag{9}$$

where we used $v(x_*) = 0$ and dropped the higher order terms in the Taylor series assuming $v'(x_*) \neq 0$. The vector field has now become a linear function of x. The solution with IC $x(0) = x_0 \approx x_*$ is

$$x(t) = x_* + (x_0 - x_*)e^{v'(x_*)t} \quad \text{for small} \quad |x - x_*|. \tag{10}$$

Thus we see that the trajectory moves away/towards x_* according as $v'(x_*)$ is positive or negative. We say the fixed point x_* is linearly unstable/stable in these two cases. When $v'(x_*) < 0$ the above solution can be trusted for all $t > 0$ and in fact becomes increasingly accurate with $x \to x_*$ as $t \to \infty$. This explains why it took infinitely long for the non-constant solutions to $\dot{x} = -\sin x$ to approach the stable fixed points. On the other hand, when $v'(x_*) > 0$, the exponentially growing solution cannot be trusted for very long, as $|x - x_*|$ would become large. Ignored nonlinear effects would become important. In the above example, this exponential growth away from the unstable fixed points is eventually superseded by *nonlinear saturation* effects as $x(t)$ approaches a stable fixed point value as $x \to \infty$.

• When $v'(x_*)$ vanishes, this linear stability analysis is inconclusive and the fixed point is said to be of marginal stability. One could include higher order terms in the Taylor expansion to try to understand its stability in a nonlinear sense.

• When $v'(x_*) \neq 0$, the characteristic time scale $1/v'(x_*)$ is the exponential growth or decay rate. It controls how quickly a trajectory leaves/approaches x_*.

2.2 More examples: RC circuit, Logistic equation

• **Example. RC circuit.** The dynamical variable is the charge $Q(t)$ that builds up on a capacitor of capacitance C, when connected in series at $t = 0$ to a resistance R and a DC battery with constant voltage V. The battery voltage V is then the sum of the voltage drops IR and Q/C across the resistor and capacitor where $I = \dot{Q}$ is the current. The resulting evolution equation is

$$\dot{Q} = \frac{V}{R} - \frac{Q}{RC} = v(Q). \tag{11}$$

There is a unique fixed point $Q_* = CV$ with the flow being towards it both from $Q > Q_*$ and $Q < Q_*$. Thus Q_* is a stable fixed point, in fact it is globally stable as the charge on the capacitor always tends asymptotically to Q_* irrespective of the initial charge. Moreover, $v'(Q_*) = -1/RC < 0$ so that the fixed point is linearly stable as we would expect. Notice that the charge Q monotonically approaches Q_*, it does not oscillate.

• **Example. Logistic equation:** The logistic equation is a simple model for the dynamics of the population $N(t)$ of a species. It postulates that the per-capita growth rate $\dot{N}/N$ is a constant $r > 0$ for small N so that small populations grow exponentially. However, as the population grows, pressure on resources leads to a decrease in the per-capita grow rate which eventually drops to zero when the population reaches the carrying capacity K. This is modeled via the ODE

$$\dot{N} = rN(1 - N/K) = v(N). \tag{12}$$

It is clear that the vector field has two zeros: at $N = 0$ and $N = K$. The flow is to the right for $0 < N < K$ where $v > 0$ and to the left for $N > K$ where $v < 0$. Draw a phase portrait. Moreover $v'(0) = r > 0$ while $v'(K) = -r$. Thus, while a zero population is an unstable fixed point, the carrying capacity is a stable fixed point: any non-zero population always tends monotonically to the carrying capacity as $t \to \infty$.

2.3 1d Flows as gradient flows and general features

1d flows as gradient flows: The lack of oscillations and monotonic approach to equilibrium in 1d flows suggests that they describe dissipative processes where some 'potential energy' is monotonically decreasing along the flow. Can we find such a monotonically decreasing function? Yes! In fact, suppose $-\phi$ is an anti-derivative for v, i.e., $v(x) = -\phi'(x)$. ϕ may be viewed as a potential energy (or velocity potential in fluid mechanics). Then the flow equation becomes

$$\dot{x} = -\phi'(x). \tag{13}$$

In other words, we have expressed the vector field as the gradient of a potential: this is always possible for vector fields on the real line. Such a flow is called a gradient flow. Now consider

$$\frac{d\phi}{dt} = \phi'(x)\frac{dx}{dt} = -\phi'(x)^2 \leq 0. \tag{14}$$

Thus we see that the potential ϕ is monotonically decreasing (non-increasing) along the flow. It is an example of a 'Lyapunov' function.

• **Main features of flows on a line:** Inspired by the examples we may now summarize some key features of 1d flows on the line. Fixed points occur at points where the graph of $v(x)$ crosses the x axis. Between successive fixed points (or between a fixed point and $\pm\infty$) v has a definite sign so that x is either increasing or decreasing. In particular, x *cannot oscillate* and there are no non-constant periodic solutions in 1d. Thus, the phase point, if it does not start at a fixed point, will approach a fixed point or $\pm\infty$ monotonically. Furthermore, the graph of x as a function of t is convex from below if $v > 0$ and $v' > 0$ or if $v < 0$ and $v' < 0$. It is concave from below if $v > 0$ and $v' < 0$ or if $v < 0$ and $v' > 0$.

Moreover, such a flow is a gradient flow with the anti-derivative of v monotonically increasing in time. We may view $\dot{x} = -\phi'(x)$ as an overdamped limit (inertia $m \to 0$) of Newton's equation $m\ddot{x} = -\gamma\dot{x} - \phi'(x)$ for a particle moving in the potential $\phi(x)$ subject to a damping force with coefficient $\gamma = 1$. By ignoring the inertia term, we have reduced the order of the equation by one and exaggerated the effect of damping, thereby eliminating the possibility of oscillations.

2.4 Existence and uniqueness

• Given the 1d vector field $v(x)$, when can we guarantee that the solution to the IVP $\dot{x} = v(x)$, $x(0) = x_0$ exists (for some time t) and is unique? Let us first give some examples that illustrate how existence and/or uniqueness can fail.

• **Failure of existence:** Let us consider the vector field

$$v(x) = \begin{cases} -c & \text{if} \quad x > 0 \\ c & \text{if} \quad x \leq 0 \end{cases} \quad \text{where} \quad c > 0 \quad \text{is a constant speed,} \tag{15}$$

and the corresponding IVP $\dot{x} = v(x)$ with $x(0) = 0$. We notice that $x = 0$ is not a fixed point, so x can't stay there. Since $v(0) = c$, the phase point wants to move to the right. However, for arbitrarily small positive x, $v(x) = -c$, so that the phase point must move to the left. These two tendencies cannot both be satisfied: there is no solution for this IC. In other words, the trajectory does not know what to do at $x = 0$. On the other hand, if we start from a non-zero

IC, say $x(0) = x_0 > 0$, then there is a solution $x(t) = x_0 - ct$. However, this solution ceases to exist at $t = x_0/c$ when the phase point approaches the origin. In this case, we may trace the lack of existence to the discontinuity of v at $x = 0$. v points in different directions as one approaches $x = 0$ from above or below. This would be okay if $v \to 0$ as $x \to 0$ so that $x = 0$ is a fixed point, but that is not the case here.

• Interestingly, discontinuous vector fields do not always fail to admit solutions to an IVP. The problem in the above example is that the flow was 'attracted' to $x = 0$, but once it got there, it did not know what to do, due to the discontinuity in v. By contrast, the discontinuous vector field

$$v(x) = c \operatorname{sgn} x = \begin{cases} c & \text{if} \quad x > 0 \\ 0 & \text{if} \quad x = 0 \\ -c & \text{if} \quad x < 0 \end{cases} \quad \text{where} \quad c > 0 \quad \text{is a constant speed,} \tag{16}$$

has solutions $(x(t) = x_0 + (\operatorname{sgn} x_0)\, ct)$ for any IC that exist for all time! $x = 0$ here is an unstable fixed point, a repeller so that trajectories are not troubled by the discontinuity at $x = 0$. Thus, while continuity may help, it is not necessary to guarantee existence of solutions.

• **Failure of uniqueness:** Consider $\dot{x} = \sqrt{x}$ for $x \geq 0$ subject to the IC $x(0) = 0$. $x = 0$ is clearly a fixed point. However, the constant solution $x(t) \equiv 0$ is not the only possibility. Indeed, integrating, and imposing the IC we find $2\sqrt{x} = t$, leading to the non-constant solution $x(t) = t^2/4$. What went wrong? Notice that the vector field v is not differentiable at $x = 0$, its derivative $v'(x) = 1/2\sqrt{x}$ diverges there. As a consequence, a linear stability analysis would say that the fixed point $x = 0$ is infinitely unstable. In fact, there are infinitely many solutions to the above IVP. Indeed, we verify that the following is a solution for any $t_0 \geq 0$:

$$x(t) = \begin{cases} 0 & \text{for } \ 0 \leq t \leq t_0 \\ (t - t_0)^2/4 & \text{for } \ t \geq t_0, \end{cases} \tag{17}$$

The first two solutions we found are the limiting cases $t_0 \to \infty$ and $t_0 = 0$. For $t_0 > 0$ we notice that the solution has a discontinuous second derivative at $t = t_0$.

It is possible to avoid this non-uniqueness if v is sufficiently regular. There are various sufficient conditions that guarantee existence and uniqueness of solutions. One of these is given in the theorem below (the proof can be found in most texts on ODEs.)

• **Existence-Uniqueness Theorem:** Suppose $v(x)$ and $v'(x)$ are continuous on an open interval containing x_0. We say that v is continuously differentiable or C^1. Then the ODE $\dot{x} = v(x)$ with $x(0) = x_0$ has a unique solution for some time interval $|t| < \tau$.

• **Picard Iteration** is a method to construct a solution to the IVP $\dot{x} = v(x)$, $x(0) = x_0$ and to prove the existence-uniqueness theorem when v is continuously differentiable. It proceeds by defining a sequence of functions $x_k(t)$ for $k = 0, 1, 2, \ldots$ inductively via

$$x_0(t) = x_0 \quad \text{and} \quad x_{k+1}(t) = x_0 + \int_0^t v(x_k(t'))\, dt' \tag{18}$$

which are then shown to converge to the solution. The idea behind this scheme is to first convert the ODE into an integral equation by integrating from 0 to t:

$$x(t) - x(0) = \int_0^t v(x(t'))\, dt' \quad \Rightarrow \quad x(t) = x_0 + \int_0^t v(x(t'))\, dt'. \tag{19}$$

This integral equation is a compact form of the IVP: it encodes both the differential equation and the IC. However, $x(t)$ appears both on the left and the right. The idea is to begin with the zeroth approximant $x_0(t) = x_0$ and use it to generate the next approximant by replacing $x(t)$ by $x_0(t)$ on the RHS. Thus $x_1(t) = x_0 + \int v(x_0(t'))dt'$. Repeating this we obtain the Picard iterates (18). Picard iteration is used to solve the time-dependent Schrödinger equation in quantum mechanics, the resulting series is called the Born series. Truncating it leads to the Born approximation. A similar procedure is employed in quantum field theory and goes by the name Dyson series.

• **Can a trajectory $x(t)$ reach or emerge from a fixed point x_* in a finite time?** In the examples $v(x) = -\sin x$, the RC circuit and the logistic equation we saw that it takes infinitely long for a solution to either reach or emerge from a fixed point. If a solution reaches or emerges from a fixed point x_* in finite time, then the IVP through x_* would have at least two solutions and would not be unique. For instance, in the above example $v = \sqrt{x}$, in addition to the constant solution $x(t) \equiv 0$ we have the non-constant solution $x(t) = t^2/4$ that emerges from the fixed point $x_* = 0$ in finite time. Alternatively, the time-reversed flow $\dot{x} = -\sqrt{x}$ with IC $x(0) = x_0 \geq 0$ has a fixed point at $x_* = 0$, which is reached by the solution $x(t) = (\sqrt{x_0} - t/2)^2$ in finite time $t_* = 2\sqrt{x_0}$.

• **Finite-time blow-ups:** Though the theorem guarantees the existence of a solution for some time, the solution need not exist for all time, it could blow up at a singularity. For example, consider the smooth vector field $v(x) = 1 + x^2$. It has no zeros and the above theorem guarantees existence and uniqueness of solutions for any initial state x_0. However, the solution $x(t) = \tan(t + \arctan x_0)$ diverges as $t + \arctan x_0$ approaches the nearest odd multiple of $\pi/2$ from below. This is an example of a finite time blow-up. Roughly, the reason this happened is that the vector field $v(x) = 1 + x^2$ grows without bound rather quickly. Notice that this did not happen for a bounded vector field like $v(x) = \sin x$ or one that grows linearly $v(x) = x$. In the latter case, the solution $x(t) = x_0 e^t$ grows but diverges only as $t \to \infty$.

• Consider the vector field on the positive real line $v(x) = x^{1+\epsilon}$ (with $x > 0$) for some $\epsilon > 0$. Find the solution with IC $x(0) = x_0 > 0$. Show that the solution blows up in finite time for any $\epsilon > 0$. Find the blow-up time.

3 Bifurcations of vector fields on the real line

• We are often interested not in a single vector field but in a family of vector fields depending continuously on a control parameter, say r. There could be more than one control parameter in a problem, they may be masses of particles or coupling constants or material constants, growth rates etc. Even in 1d, the nature of fixed points and the structure of the phase portrait can undergo qualitative changes (known as 'bifurcations') as the control parameter is varied across a critical value r_c, the bifurcation point. Bifurcations are like phase transitions.

• For instance, at a bifurcation, fixed points may be created or destroyed or their stability may change.

• We will examine three types of bifurcations in 1d: saddle-node, transcritical and pitchfork.

• The buckling/bending of a horizontal rectangular card compressed between two opposite edges using two fingers provides an example. The compressional stress is the control parameter while a measure of departure of the card from flatness (e.g. height of center relative to compressed edges)

is the dynamical variable. For a range of small compressional forces, the card has only one stable equilibrium: it is flat. At a critical compression, it bends either upwards or downwards. Thus, for compression above the threshold value, we have two stable equilibria (cards bent upwards or downwards) and one unstable equilibrium (flat card). This is an example of a pitchfork bifurcation. It is associated with spontaneous breaking of the up-down reflection symmetry.

• The transition from laminar to turbulent flow of a fluid or plasma can involve bifurcations.

3.1 Saddle-node bifurcation

• In a saddle-node bifurcation, two fixed points merge and annihilate leaving no fixed point, as a control parameter is increased across r_c. Decreasing r across r_c would describe the 'pair production' of two fixed points from a situation where there are no fixed points. The name saddle-node bifurcation comes from the generalization of this bifurcation to flows on the plane.

• The prototypical family of vector fields displaying such a bifurcation is $v(x;r) = r + x^2$. The bifurcation point is $r_c = 0$. Notice that for $r < 0$, v has two fixed points: $x = \sqrt{-r}$ is unstable while $x = -\sqrt{-r}$ is stable. They coalesce at the half-stable fixed point $x = 0$ as $r \to 0^-$. For $r > 0$ there are no fixed points. Draw a *bifurcation diagram* showing the locations of the fixed points on the r-x plane (with r along the horizontal axis). It should indicate why a saddle-node bifurcation is also called a fold or turning point bifurcation.

• Similarly, $v(x;r) = r - x^2$ displays a saddle-node bifurcation where a pair of fixed points emerge as r increases beyond $r_c = 0$.

• The above quadratic vector fields are not just simple examples, they are canonical/normal forms of vector fields displaying a saddle-node bifurcation (in the neighborhood of the bifurcation point and in the vicinity of the merging fixed points). Indeed, without loss of generality we may take the bifurcation point to be $r_c = 0$ and the point of coalescence of fixed points to be $x = 0$. Then $v(x;r)$ must be parabolic in x for x and r near zero in order for there to be two merging fixed points. This may also be seen by Taylor expanding a vector field $v(x;r)$ that displays a saddle-node bifurcation at (x_*, r_c). Indeed,

$$v(x;r) = v(x_*;r_c) + (x-x_*)\partial_x v(x_*;r_c) + (r-r_c)\partial_r v(x_*;r_c) + \frac{1}{2}(x-x_*)^2\partial_x^2 v(x_*;r_c) + \cdots . \quad (20)$$

Now $v(x_*, r_c) = 0$ as x_* is a fixed point when $r = r_c$. Moreover, $\partial_x v(x_*;r_c) = 0$ as the graph of v must be tangent to the x-axis when $r = r_c$ so that v can have a double zero corresponding to the coalescence of fixed points. Neglecting higher order terms, we get the canonical form $v(x;r) = a(r-r_c) + b(x-x_*)^2$.

3.2 Transcritical bifurcation

This describes a situation where a fixed point x_* exists for all parameter values, but whose stability changes as r is varied. For instance, x_* may go from being stable to unstable as r crosses r_c. This is achieved by making another fixed point 'pass through' x_* and 'exchange stabilities' with it. The following normal form demonstrates the phenomenon. Consider

$$v(x) = rx - x^2 = x(r-x) = -(x - r/2)^2 + r^2/4. \quad (21)$$

$x_* = 0$ is clearly always a fixed point. A second fixed point located at $x_{**} = r$ moves to the right as r increases past $r_c = 0$. Graph $v(x)$ for various values of r to see the following. For $r < 0$, the fixed point at the origin is stable while the one at r is unstable. At $r = 0$, $v = -x^2$ and the fixed points merge at the origin which is half-stable. Finally, for $r > 0$ the origin becomes unstable while $x_{**} = r$ is stable. Thus, the fixed points have exchanged stabilities via the bifurcation at $r = 0$. Indicate the locations of the fixed points as a function of r on a bifurcation diagram.

• The logistic equation, now considered for real N, K and r,

$$\dot{N} = rN(1 - N/K) = (r/K)N(K - N), \tag{22}$$

displays a transcritical bifurcation of the $N_* = 0$ (zero population) fixed point as the carrying capacity K slides past $K_c = 0$ provided $\tilde{r} = r/K > 0$ is held *fixed*. For $K < 0$, $N_* = 0$ is stable as $v'(0) = K\tilde{r} < 0$ while $N_* = K$ is unstable. The two fixed points exchange stabilities at $K_c = 0$ with the zero population fixed point becoming unstable and $N_* = K$ becoming stable for $K > 0$.

• There are variants of this transcritical bifurcation where the stability of a fixed point changes as a parameter is varied.

1. For instance, for the linear vector field $v(x) = rx$, $x_* = 0$ changes from being stable for $r < 0$ to unstable for $r > 0$. At $r = 0$ we have a line of fixed points: the vector field vanishes. Draw the bifurcation diagram.

3.3 Pitchfork bifurcations

Pitchfork bifurcations are named after an agricultural tool. The latter looks like a *trishul* or trident, it has a long handle and three tines or prongs. Pitchfork bifurcations are typically seen in systems with a discrete parity or left-right ($\mathbb{Z}/2\mathbb{Z} = \mathbb{Z}_2$) symmetry. In the bending of a card mentioned earlier, one stable flat (parity invariant) equilibrium configuration becomes unstable at the bifurcation point (critical compressional stress) where two stable equilibria with opposite parities are born. Though the word bifurcation is standard, pitchfork trifurcation describes the situation more accurately.

• There are two types of pitchfork bifurcations: supercritical and subcritical. The former is associated with the bending of a card or buckling of a column under a weight as well as to second order or continuous phase transitions while the latter is associated with first order or discontinuous phase transitions in thermal physics.

3.3.1 Supercritical pitchfork bifurcation

The normal form in this case is

$$\dot{x} = rx - x^3 = x(r - x^2) \tag{23}$$

This ODE has an $x \to -x$ parity symmetry. This means that every trajectory is either parity neutral or comes paired with another trajectory related to it by a parity transformation. This applies to fixed points as well (which are static trajectories). For $r < 0$, the origin $x = 0$ is the

only fixed point, and it is stable. $v'(0) = r$ so that trajectories approach the origin exponentially fast with time constant $1/r$. When $r = 0$, the vector field has a triple zero at $x = 0$, which is still a stable fixed point, though the linear decay time constant diverges. So trajectories that start at x_0 at $t = 0$, i.e., $x(t) = \text{sgn}\,(x_0)\,(2t + 1/x_0^2)^{-1/2}$ approach the origin like a power-law rather than exponentially fast. This is similar to critical slowing-down in the vicinity of a 2nd order phase transition in classical statistical mechanics. Finally, when $r > 0$, we have three fixed points, an unstable one at $x = 0$ and two stable 'non-trivial' fixed points at $x = \pm\sqrt{r}$. A bifurcation diagram on the r-x plane showing the fixed points looks like a horizontal pitchfork with prongs pointing to the right. The connection to the bending of a card is evident. This pitchfork bifurcation is called *supercritical* to signify that the nontrivial fixed points that are born at the bifurcation are stable (also, two nontrivial fixed points exist only above the critical point if r is increased.).

• It is instructive to look at the potential for the vector field $v(x) = rx - x^3$. It is a quartic potential $\phi(x) = -\frac{1}{2}rx^2 + \frac{1}{4}x^4$ with $v = -\phi'$. Viewed as a potential for a particle moving on the line, we see that the quartic term is attractive/stabilizing. For $r < 0$, ϕ has only one extremum, a global minimum at $x_* = 0$, the minimum becomes very flat $\phi = x^4/4$ at the critical point $r = 0$ while it turns into a double-well potential for $r > 0$.

• The *basin of attraction* of a fixed point x_* is the set of ICs x_0 for which $x(t) \to x_*$ as $t \to \infty$. If the basin of attraction is the whole phase space, we say that x_* is a global attractor. In the above case, $x_* = 0$ is a global attractor for $r \leq 0$. For $r > 0$, the two fixed points $x_* = \pm\sqrt{r}$ have basins of attraction consisting of the positive and negative half lines $x_0 > 0$ and $x_0 < 0$, while $x_0 = 0$ is the only point in the basin of attraction of the unstable fixed point at $x_* = 0$.

• A system with a $\mathbb{Z}_2$ symmetry displaying a second order phase transition is a 2d Ising spin system where 'spins' which can either point up or down are located on a square lattice. Neighboring spins tend to align due to the exchange interaction but thermal fluctuations can prevent all spins from being aligned the same way. The system as a whole is invariant under reversal of the sign of all spins. The system displays a 2nd order paramagnetic to ferromagnetic transition as the temperature (control parameter) is lowered below the Curie temperature T_c. In the paramagnetic phase the net magnetization ($\propto$ total spin) is zero (due to thermal fluctuations) corresponding to the single fixed point $x_* = 0$. In the ferromagnetic phase there is a non-zero net 'spontaneous' magnetization with all spins in a magnetic domain pointing either up or down (corresponding to the stable fixed points $x_* = \pm\sqrt{r}$). In the vicinity of the 2nd order phase transition at T_c, there are long-range fluctuations, one of whose effects is that one needs to average over a very large number of configurations to reliably calculate mean values in a Gibbs ensemble. This is one manifestation of critical slowing down. Moreover, correlation functions decay as a power law at the critical temperature while away from the critical temperature, they decay exponentially.

3.3.2 Subcritical pitchfork bifurcation

Reversing the sign of the quartic term in the potential ϕ or the cubic term in v leads to a subcritical pitchfork bifurcation. Thus we consider

$$\dot{x} = rx + x^3 = x(r + x^2) \tag{24}$$

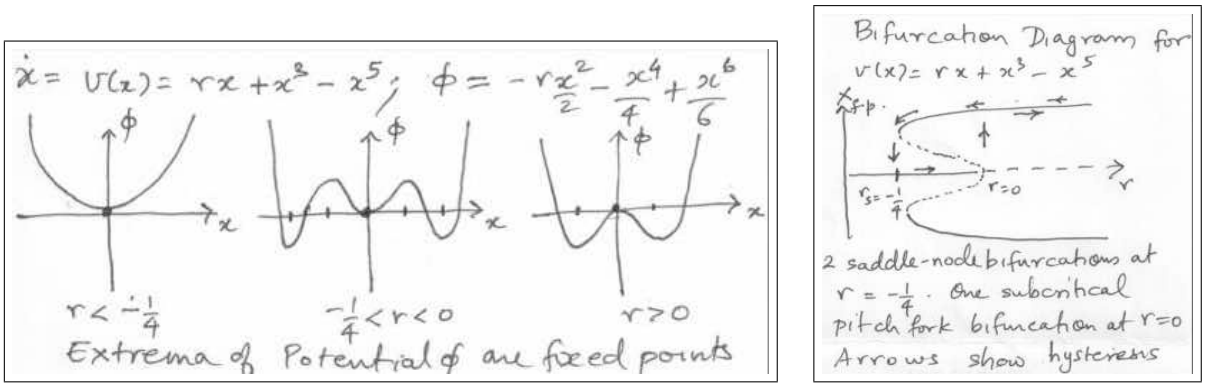

Figure 2: Potential and Bifurcation diagram for $\dot{x} = v(x) = rx + x^3 - x^5$.

which corresponds to the quartic potential $\phi(x) = -\frac{1}{2}rx^2 - \frac{1}{4}x^4$. For $r < 0$, there are three fixed points $x_* = 0$ (stable) and $x_* = \pm\sqrt{-r}$ (unstable). When $r \to 0^-$ the three fixed points merge into a single unstable fixed point at $x_* = 0$ which then survives as an unstable fixed point for $r > 0$. The bifurcation diagram for a subcritical pitchfork bifurcation looks like a laterally inverted version of the supercritical one, except that the non-trivial fixed points are unstable in the subcritical case, while they were stable in the supercritical case. It is called a subcritical pitchfork bifurcation to convey that the nontrivial fixed points $x_* = \pm\sqrt{-r}$ are unstable (also, the non-trivial fixed points exist only for r below the critical value $r_c = 0$ for our setup). What is more, for $r \geq 0$, the origin is very unstable and all non-constant trajectories blow-up in finite time. This is easily seen for $r = 0$ where the solution to the IVP is $x(t) = \text{ sgn } (x_0)(1/x_0^2 - 2t)^{-1/2}$. We see that $x(t) \to \pm\infty$ according as $\text{ sgn } (x_0) = \pm 1$ at the blowup time $t_b = 1/2x_0^2$ for any non-zero x_0.

• In practice, additional nonlinear effects would become important once the solutions grow sufficiently. The simplest model incorporating these (that retains the $x \to -x$ symmetry) is

$$\dot{x} = v(x) = rx + x^3 - x^5. \tag{25}$$

It is clear that $x_* = 0$ is always a fixed point, it is linearly stable for $r < 0$ and unstable for $r > 0$. The other fixed points are roots of the quartic equation $r + x^2 - x^4 = 0$. They are at

$$x_*^{\pm\pm} = \pm\left[\frac{1}{2}(1 \pm \sqrt{1 + 4r})\right]^{1/2}. \tag{26}$$

For $r < r_s = -1/4$, $x_* = 0$ is the only fixed point. For $-1/4 < r < 0$ there are four non-trivial fixed points $x_*^{\pm\pm}$. While $x_*^{\pm,-}$ are unstable, $x_*^{\pm,+}$ are stable. For $r > 0$ we have only two non-trivial fixed points $x_*^{\pm,+}$, both of which are stable. This vector field displays both a subcritical pitchfork bifurcation at $r = 0$ as well as a pair of saddle-node bifurcations at $r_s = -1/4$ where the stable $(x_*^{\pm,+})$ and unstable $(x_*^{\pm,-})$ large-amplitude fixed points are born. Draw the bifurcation diagram.

• It is also instructive to draw the potential $\phi(x) = -rx^2/2 - x^4/4 + x^6/6$ in the three qualitatively different regions: (a) $r < -1/4$, (b) $-1/4 < r < 0$ and (c) $r > 0$. For $r < -1/4$, the quartic term does not have a chance to play a qualitative role (for small x it is dominated by the quadratic term with large coefficient, while for large x it is dominated by the x^6 term!)

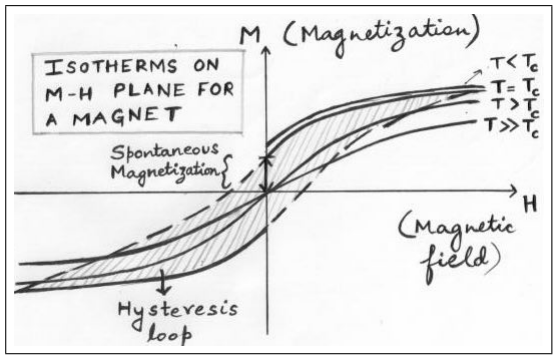

Figure 3: Plot of magnetization vs applied magnetic field for various temperatures in a magnetic domain. For $T > T_c$ (paramagnetic phase) $M = \chi H$ for small H (linear response regime) while M saturates for large H. For $T \leq T_c$ (ferromagnetic phase) there is a residual (spontaneous) magnetization even when $H \to 0^{\pm}$. The memory effect (hysteresis loop) is also shown. Thanks to Sonakshi Sachdev for help with the Figure.

and ϕ has only one extremum, a global minimum at $x_* = 0$. For $-1/4 < r < 0$, there is a local minimum at $x_* = 0$, a pair of local maxima at $x_*^{\pm,-}$ and a pair of global minima at $x_*^{\pm,+}$. Finally, for $r > 0$, ϕ has a local maximum at $x_* = 0$ and a pair of global minima at $x_*^{\pm,-}$.

• Interestingly, this system can display jumps and hysteresis. Thus, unlike the supercritical bifurcation that is associated to second order (continuous) phase transitions, the subcritical one is associated to first order (discontinuous) phase transitions. Indeed, suppose we begin with the system in its unique stable equilibrium $x_* = 0$ for $r < -1/4$ and imagine slowly increasing r. As the trivial fixed point is linearly stable up to $r = 0^-$, the system remains at $x_* = 0$. At $r = 0$, the slightest perturbation causes the system to make a discontinuous transition or 'jump' from $x_* = 0$ to one of the two stable fixed points $x_* = x_*^{\pm,+}$. Suppose it jumps to the 'upper' branch $x_*^{+,+}$. With further increase in r the system remains in the stable equilibrium $x_*^{+,+}$. Now suppose r is decreased. Interestingly, the system remains in the state $x_*^{+,+}$ even when r is decreased below $r = 0$, as it is a stable state. In other words, the system does not retrace its path even when the control parameter retraces its path! Hysteresis is the name for this lack in reversibility, it is seen in magnets and are associated to first order phase transitions. A second jump occurs when r is decreased down to $r_s = -1/4$ at which point the non-trivial fixed points cease to exit and the system jumps back to the stable equilibrium $x_* = 0$. Draw a figure.

4 Vector fields on a circle

Vector fields on a circle will provide us the simplest examples of dynamical systems that can display oscillations.

• The integral curves of a vector field $v(\theta)$ on a circle are solutions of the first order ODE $\dot{\theta} = v(\theta)$. Here, the 2π-periodic coordinate θ parametrizes points on a circle, with θ increasing counter-clockwise. In particular, $v(\theta)$ must be 2π-periodic so that the vector field is single-valued.

• **Uniform circular motion:** The constant vector field $v(\theta) = \omega$ (for $\omega \neq 0$) describes uniform oscillations. Indeed, the solution to the IVP $\theta = \theta_0 + \omega t$ describes a phase point rotating uniformly (counter-clockwise if $\omega > 0$ and clockwise if $\omega < 0$) at angular velocity ω.

Notice that this vector field has no fixed points! The phase point returns to its initial location after a time period $T = 2\pi/|\omega|$. ω represents a constant torque that drives the phase point round and round.

• **Overdamped pendulum:** The example $\dot{x} = -\sin x$ considered earlier is in fact better viewed as a dynamical system on the circle. If we regard $x = \theta$ as an angle then $\theta = 0, \pi \pmod{2\pi}$ are the only fixed points, they lie at the bottom and top of the circle. The flow is clockwise on the right semi-circle and counter-clockwise on the left. Thus $\theta = 0$ is stable while $\theta = \pm\pi$ is unstable. In this case, all trajectories other than the constant one at $\theta = \pi$ eventually end up at the attractive fixed point $\theta = 0$. There is no oscillatory behavior and no non-trivial periodic solutions exist. The equation describes an overdamped pendulum. $\theta = 0$ is the stable equilibrium with bob hanging down and $\theta = \pi$ is the unstable equilibrium with bob pointing upwards.

• **Overdamped pendulum subject to constant torque:** Let us now 'combine' the above two examples and consider the vector field

$$\dot{\theta} = \omega - a \sin\theta \tag{27}$$

with $\omega \geq 0$ and $a \geq 0$. This equation arises in the overdamped limit of a pendulum driven by a constant torque τ:

$$ml^2\ddot{\theta} = -\gamma\dot{\theta} + \tau - mgl\sin\theta, \tag{28}$$

as well as in other contexts (e.g. Josephson junctions and charge density waves, see Strogatz). We may think of ω as a measure of the counter-clockwise torque and of a as a measure of the downward acceleration due to gravity, which tries to make the bob come down to $\theta = 0$. On the other hand, ω drives the bob uniformly counterclockwise. For definiteness, we will hold $\omega > 0$ fixed and imagine increasing the control parameter a. When the gravitational force is absent ($a = 0$), we have uniform circular motion at frequency ω and time period $2\pi/\omega$. When $0 < a < \omega$, the motion around the circle becomes non-uniform. Draw a phase portrait and plot $v(\theta)$. Since $v(\theta) > 0$, the motion is still counterclockwise and periodic: there are no fixed points. The constant torque opposes gravity maximally at the bottleneck around $\theta = \pi/2$ where the bob slows down. The two forces reinforce each other most at $\theta = -\pi/2$ where the bob speeds up. For $a \ll \omega$ the non-uniformity is small. When $a \lesssim \omega$, the pendulum moves very slowly near $\theta = \pi/2$ but covers the rest of the circle quickly. At $a = a_c = \omega$, a half-stable fixed point is born at $\theta = \pi/2$ in a saddle-node bifurcation. Draw the corresponding phase portraits. For $a > \omega$, we have two fixed points $\theta_*^{\pm}$ on either side of $\theta = \pi/2$ at $\sin\theta_* = \omega/a$. Show (using linear stability analysis) that θ_*^+ (the one to the right of $\pi/2$) is unstable while the one to its left (θ_*^-) is stable. In this phase, the motion is no longer oscillatory and all non-constant trajectories are attracted to the stable fixed point θ_*^- whose basin of attraction is the circle with θ_*^+ removed.

5 Linear vector fields on the plane and their fixed points

Non-constant integral curves of vector fields on the plane display richer behavior (e.g. periodicity, oscillations, limit cycles, homo and heteroclinic orbits etc) than on a line where they had to monotonically approach a stable fixed point or $\pm\infty$ without oscillation or the possibility of periodic motion. We will begin by examining linear systems in 2d as they are simpler and also help to classify fixed points of more general flows on a plane.

• A (homogeneous) linear vector field on the plane $\mathbf{v} = A\mathbf{r}$, where $\mathbf{r}$ is a 2-component vector and A a 2×2 real (not necessarily symmetric) matrix leads to the 2d homogeneous linear system

$$\begin{pmatrix} \dot{x} \\ \dot{y} \end{pmatrix} = \begin{pmatrix} a & b \\ c & d \end{pmatrix} \begin{pmatrix} x \\ y \end{pmatrix} \quad \text{or} \quad \dot{\mathbf{r}} = \mathbf{v} = A\mathbf{r}. \tag{29}$$

The IVP now requires two initial conditions $x(0)$ and $y(0)$. It is clear that the origin $\mathbf{x}_* = (0, 0)$ is always a fixed point. There could be non-trivial fixed points $\mathbf{r}_* \neq 0$ with $A\mathbf{r}_* = 0$, if A is singular (i.e. if $\det A = 0$ or equivalently if it has a non-trivial kernel or null-space). More precisely, the origin is the only fixed point if $\det A \neq 0$, we have a line of fixed points along the null space of A if the null space is one-dimensional and a plane of fixed points if A has a two-dimensional null-space (in which case $A = 0$). The trajectories are directed parametrized curves $(x(t), y(t))$ on the x-y phase plane whose velocity vector is $\mathbf{v}$. Poincaré classified the possible phase portraits of such systems. Let us begin with some examples that illustrate the types of fixed points that can occur.

• It is noteworthy that the time-dependent Schrödinger equation of quantum mechanics $i\hbar\dot{\psi} = H\psi$ is a linear equation of the above sort, with the Hamiltonian operator H defining a vector field on the state space. However, the state space in QM is in general a complex vector space whose dimension could be finite or infinite and H is restricted to be hermitian.

5.1 Examples of fixed points: center, node, saddle

• **Center (simple harmonic oscillator):** Linear systems in 2d naturally arise when studying the Newtonian dynamics of a particle moving on a line subject to a linear force. In the language of mechanics, such systems have one degree of freedom and a two-dimensional phase space. A familiar example is the simple harmonic oscillator $m\ddot{x} = -kx$ that arises in describing small oscillations of amplitude x, of a mass m attached to a spring with force constant k. Introducing the linear momentum $p = m\dot{x}$ we write this as the pair of coupled linear equations for the coordinates (x, p) on the phase plane

$$\begin{pmatrix} \dot{x} \\ \dot{p} \end{pmatrix} = \begin{pmatrix} p/m \\ -kx \end{pmatrix} = \begin{pmatrix} 0 & 1/m \\ -k & 0 \end{pmatrix} \begin{pmatrix} x \\ p \end{pmatrix}. \tag{30}$$

In this case, the coefficient matrix is non-singular ($\det A = k/m = \omega^2 > 0$) so that the origin is the only fixed point. It corresponds to the static solution ($x = p = 0$) where the mass is always at rest. More generally, show that the phase trajectories are clockwise-directed closed curves centered at the origin and display them on a phase portrait. These periodic trajectories describe an oscillating mass. In fact, the general solution to the above ODEs is

$$x(t) = A\cos(\omega t + \varphi) \quad \text{and} \quad p(t) = -m\omega A \sin(\omega t + \varphi) \tag{31}$$

where φ and A are constants determined by initial conditions. Unlike with flows on a line, which had to be gradient flows with a monotonically decreasing 'potential energy', this is a conservative system. It is easily verified that the energy or Hamiltonian $H = p^2/2m + kx^2/2$ is constant along trajectories. In fact, the trajectories coincide with the level curves of H, which are ellipses.

What is the nature of the fixed point $\mathbf{r}_*$ at the origin? It is called a center or an elliptic fixed point or an O-point. It is neither an attractive fixed point nor a repulsive one: trajectories that

begin nearby do not approach it nor go away from it asymptotically (as $t \to \infty$). However, a trajectory that begins nearby remains nearby: this is called Lyapunov stability, after the Russian mathematical physicist. Furthermore, we say that the fixed point at the origin is neutrally stable since it is Lyapunov stable but not attracting. Coincidentally, the matrix A is not diagonalizable over the reals: it has purely imaginary eigenvalues ($\pm i\omega$). We will see later how this is related to the stability of $\mathbf{r}_* = 0$.

• We have introduced two notions of stability here. The first concerns asymptotic behavior: a fixed point $\mathbf{r}_*$ is said to be attractive if trajectories that begin sufficiently close to $\mathbf{r}_*$ approach $\mathbf{r}_*$ as $t \to \infty$. On the other hand, Lyapunov stability concerns behavior at all times: $\mathbf{r}_*$ is Lyapunov stable if trajectories that begin sufficiently close to $\mathbf{r}_*$ remain close to $\mathbf{r}_*$ at all subsequent times[3]. A fixed point that is both attracting and Lyapunov stable is called asymptotically stable. Though the two often occur together, they need not. The origin in the harmonic oscillator is Lyapunov stable but not attracting. On the contrary, a fixed point may be attracting but not Lyapunov stable, if trajectories that begin nearby go far away before eventually reaching $\mathbf{r}_*$. An example is given by the half-stable fixed point $\theta_* = \pi/2$ of the vector field $v(\theta) = \omega(1 - \sin\theta)$ on the circle. It is attracting, since all trajectories eventually approach $\theta = \pi/2$. However, it is not Lyapunov stable as the trajectories have to go 'round the circle' before eventually falling into the fixed point.

• **Node, star, saddle and line of fixed points:** Consider the family of linear systems on the plane parametrized by a real number α:

$$\begin{pmatrix} \dot{x} \\ \dot{y} \end{pmatrix} = \begin{pmatrix} \alpha & 0 \\ 0 & -1 \end{pmatrix} \begin{pmatrix} x \\ y \end{pmatrix} \quad \text{with} \quad x(0) = x_0 \quad \text{and} \quad y(0) = y_0. \tag{32}$$

As long as $\alpha \neq 0$, the origin is the only fixed point. When $\alpha = 0$, every point on the x axis is a fixed point. In both cases, the equations decouple and the solutions are easily written down:

$$x(t) = x_0 e^{\alpha t} \quad \text{and} \quad y(t) = y_0 e^{-t}. \tag{33}$$

It is clear that y monotonically decays to zero while the behavior of x depends on α. Draw the phase portrait for five values of α: $\alpha < -1$, $\alpha = -1$, $-1 < \alpha < 0$, $\alpha = 0$ and $\alpha > 0$. (i) When $\alpha < -1$ the origin is the only fixed point. All non-constant trajectories approach it while becoming asymptotically tangent to the y-axis, as x decays faster than y. The fixed point at the origin is called a stable node. It is both Lyapunov stable and attracting and therefore asymptotically stable. (ii) When $\alpha = -1$, $A = -I$ and x and y approach zero at the same rate. All non-constant trajectories are straight lines that approach the origin as $t \to \infty$. The origin is still an asymptotically stable node but in this case it is called a symmetrical node or star. (iii) For $-1 < \alpha < 0$ the origin remains an asymptotically stable node, but with trajectories approaching it along the x-axis as y decays faster. (iv) If $\alpha = 0$, x is independent of time and we have a line of fixed points along the x axis. Non-constant trajectories are vertical lines approaching one of these fixed points either from the upper or lower half plane. Each of these fixed points $\mathbf{r}_*$ is neutrally stable (Lyapunov stable but not attracting), as trajectories that

[3]More precisely, $\mathbf{r}_*$ is Lyapunov stable if given any tolerance $\epsilon > 0$ there exists a $\delta > 0$ so that we can guarantee that $|\mathbf{r}(t) - \mathbf{r}_*| < \epsilon$ for all $t > 0$ provided we start close enough ($|\mathbf{r}(0) - \mathbf{r}_*| < \delta$). If we do not have notions of distance but only the topological notion of open sets, this condition can be formulated in terms of open neighborhoods. $\mathbf{r}_*$ is Lyapunov stable if given any non-empty neighborhood N of $\mathbf{r}_*$, there exists a non-empty neighborhood V of $\mathbf{r}_*$ such that if the initial condition lies within V then $\mathbf{r}(t)$ is guaranteed to lie within N for all $t \geq 0$.

begin nearby remain nearby but may not approach $\mathbf{r}_*$. (v) Finally, when $\alpha > 0$, the fixed point at the origin is a saddle point, also called an X-point. It is an example of what is called a hyperbolic fixed point[4]. Trajectories with $x_0 = 0$ approach it along the y axis. But all other non-constant trajectories asymptotically approach $(x = \pm\infty, y = 0)$. Thus, the saddle point is neither Lyapunov stable nor attractive. For $\alpha = 1$, the phase portrait consists of a family of hyperbolae with xy constant (in general xy^α is constant on trajectories). For a saddle point (and more generally for hyperbolic fixed points), one defines the notions of stable and unstable manifolds. The stable manifold W_s of a hyperbolic fixed point $\mathbf{r}_*$ is defined as the set of ICs (x_0, y_0) (points on phase space) for which the trajectory tends to $\mathbf{r}_*$ as $t \to \infty$. The unstable manifold W_u is similarly the set of ICs for which the trajectory tends to $\mathbf{r}_*$ as $t \to -\infty$. In the case at hand, W_s is the y-axis while W_u is the x-axis. We observe that a typical trajectory (in this case, every trajectory) approaches the unstable/stable manifold as $t \to \pm\infty$.

5.2 Analysis of phase portrait using eigenvalues and eigenvectors of coefficient matrix

• One reason we could easily analyze the second example above is that the equations for x and y decoupled as A was a diagonal matrix. The horizontal and vertical directions were eigendirections of A. In general, an IC in an eigendirection leads to simple evolution. Suppose $\mathbf{w}$ is a (real) eigenvector of A with (real) eigenvalue λ, $A\mathbf{w} = \lambda\mathbf{w}$. Then if the initial state $\mathbf{r}(0) = r_0\mathbf{w}$ is in this eigendirection, then the trajectory remains along $\mathbf{w}$ at all times. Indeed, we see that the solution is given by $\mathbf{r}(t) = e^{\lambda t} r_0 \mathbf{w}$ since $\dot{\mathbf{r}} = \lambda\mathbf{r}(t)$ is the same as $A\mathbf{r}(t)$.

• A **with two linearly independent eigenvectors:** Somewhat more generally, suppose the real matrix $A = (ab|cd)$ has two distinct eigenvalues

$$\lambda_\pm = \frac{1}{2}\left[(a+d) \pm \sqrt{(a+d)^2 - 4(ad-bc)}\right]. \tag{34}$$

Then we are guaranteed[5] that the corresponding eigenvectors $\mathbf{w}_\pm$ are linearly independent. Thus, if we expand the initial state as $\mathbf{r}_0 = r_-\mathbf{w}_- + r_+\mathbf{w}_+$, then we can immediately write down the solution to the IVP:

$$\mathbf{r}(t) = r_- e^{\lambda_- t}\mathbf{w}_- + r_+ e^{\lambda_+ t}\mathbf{w}_+. \tag{35}$$

Notably, this formula works even if the eigenvalues and eigenvectors are not real! However $\mathbf{r}_0$ must be real; a convenient way of ensuring this is to exploit the fact that $\lambda_\pm$ must be complex conjugates to take $\mathbf{w}_\pm$ to also be complex conjugates and $r_+ = r_-^*$. An immediate consequence is that if the real parts of the eigenvalues $\lambda_\pm$ are negative, then the origin is an attractor while it is unstable if $\Re\lambda_\pm > 0$. However, when the eigenvalues are not real, the eigenvectors are also not real and the corresponding eigenspaces are not lines through the origin on the plane; they cannot be interpreted as invariant subspaces for the dynamics on the plane.

On the other hand, if the eigenvalues are real, then the eigenvectors can be taken real and define invariant subspaces for the dynamics on the phase plane. They are unstable/stable depending on whether the corresponding eigenvalue is positive/negative. (a) If both are of the

[4]Somewhat confusingly, the name hyperbolic fixed point is used for a wider class of fixed points that includes saddles, nodes and spirals, as we will clarify in the next section.

[5]Suppose $A\mathbf{v} = \lambda\mathbf{v}$ and $A\mathbf{w} = \mu\mathbf{w}$ are two (non-zero) eigenvectors corresponding to distinct eigenvalues $\lambda \neq \mu$. Suppose $\mathbf{v} = \alpha\mathbf{w}$ are linearly dependent. Then $A\mathbf{v} = \lambda\mathbf{v}$ and also $A\mathbf{v} = A\alpha\mathbf{w} = \alpha\mu\mathbf{w} = \mu\mathbf{v}$ so that $(\lambda - \mu)\mathbf{v} = 0$ or $\lambda = \mu$, contradicting the hypothesis.

same sign, the origin is either a stable or unstable **node**. (b) It is a **saddle point** if they have opposite signs. (c) If $\lambda_+ = \lambda_- \neq 0$, and they nevertheless have linearly independent eigenvectors, then $A = \lambda_+ I$ and we have a stable/unstable **star or symmetrical node** depending on whether the eigenvalues are positive or negative. (d) If one eigenvalue, say λ_- is zero and the other is non-zero, then we have a **line of fixed points** along the 0-eigenspace. The fixed points are stable if $\lambda_+ < 0$ and unstable if $\lambda_+ > 0$. (e) Perhaps not surprisingly, if both eigenvalues vanish but A has two linearly independent eigenvectors, then A must be the zero matrix and **every point on the plane is a neutrally stable fixed point**.

(f) On the other hand, if the eigenvalues are purely imaginary $\lambda_\pm = \pm i\omega$, then the trajectory

$$\mathbf{r}(t) = r_- e^{-i\omega t}\mathbf{w}_- + r_+ e^{i\omega t}\mathbf{w}_+ \tag{36}$$

is periodic with period $2\pi/\omega$, as in the case of the harmonic oscillator and the origin is a **neutrally stable center**. In fact, for the SHO $A = (0, 1/m| - k, 0)$ has eigenvalues $\pm i\omega$ where $\omega = \sqrt{k/m}$. The corresponding eigenvectors can be taken as $\mathbf{w}_\pm = (1, \pm im\omega)^t$. We notice that the eigenvectors cannot be taken real, so they do not define invariant subspaces on the x-p phase plane. However, reality of A implies that $\mathbf{w}_\pm$ can be taken to be complex conjugates so that reality of $\mathbf{r}$ then implies that $r_\pm$ must also be complex conjugates. The solution $\mathbf{r} = (x, p)$ in the case of the SHO can then be written as

$$\begin{aligned} x(t) &= r_+(\cos\omega t + i\sin\omega t) + r_-(\cos\omega t - i\sin\omega t) = 2(\Re r_+)\cos\omega t - 2(\Im r_+)\sin\omega t \quad \text{and} \\ p(t) &= 2m\omega\left[-\Re r_+ \sin\omega t - \Im r_+ \cos\omega t\right]. \end{aligned} \tag{37}$$

Summing the squares we find that $(x/2)^2 + (p/2m\omega)^2$ is a constant (depending on the complex number r_+, which is determined by the ICs). Thus, the trajectories of the SHO are ellipses centered at the origin.

(g) **Spiral sink or source:** A center is not structurally stable. What this means is that a center is generally nor preserved under a perturbation of system parameters a, b, c and d. Typical perturbations (that preserve the reality of A) would cause the pure imaginary eigenvalues to move off the imaginary axis and become truly complex and conjugate to each other. In fact, if the eigenvalues are not real or imaginary, they must be of the form $\lambda_\pm = \gamma \pm i\omega$ (with $\gamma, \omega \neq 0$). The solution is then given by

$$\mathbf{r}(t) = e^{\gamma t}\left(r_- e^{-i\omega t}\mathbf{w}_- + \mathbf{r}_+ e^{i\omega t}\mathbf{w}_+\right) \tag{38}$$

In this case, we have a stable or unstable spiral (**spiral sink or source**, sometimes called a **focus**) according as γ is negative or positive. γ is called the growth or decay rate. Physically, the motion is like that of an underdamped oscillator.

5.2.1 Damped harmonic oscillator

This gives us an opportunity to take a quick look at the damped harmonic oscillator defined by Newton's equation for a particle whose displacement from equilibrium is denoted x:

$$m\ddot{x} = -kx - \gamma\dot{x}. \tag{39}$$

The linear restoring force is $-kx$ and we define the frequency $\omega = \sqrt{k/m}$ as before. Here γ is the damping coefficient, it must be positive to ensure that the damping force acts in a direction

opposite to the instantaneous velocity, thereby slowing the particle down. Introducing $p = m\dot{x}$, (39) can be written as a first order system on the x-p phase plane

$$\begin{pmatrix} \dot{x} \\ \dot{p} \end{pmatrix} = \begin{pmatrix} 0 & 1/m \\ -k & -\gamma/m \end{pmatrix} \begin{pmatrix} x \\ p \end{pmatrix}, \tag{40}$$

with initial conditions $x(0) = x_0$ and $p(0) = p_0$. The eigenvalues of the coefficient matrix are

$$\lambda_\pm = \frac{1}{2m}\left(-\gamma \pm \sqrt{\gamma^2 - 4m^2\omega^2}\right). \tag{41}$$

It is useful to note that $\det A = \lambda_+\lambda_- = \omega^2$ where A is the above coefficient matrix. Since $\Re\lambda_\pm = -\gamma/2m < 0$, the origin is an attractor: the particle eventually comes to rest at the equilibrium point $x = 0$. There are three qualitatively different parameter regimes.

1. If $\gamma < 2m\omega$ (weak damping), then, $\lambda_\pm$ are complex and the origin is a spiral sink. The motion is said to be **underdamped**: x oscillates infinitely often (with 'time period' $2\pi/|\Im\lambda_\pm| = 4\pi m/\sqrt{4m^2\omega^2 - \gamma^2}$) with decreasing amplitude as it settles down to $x = 0$. The phase trajectory winds clockwise around the origin.

2. When $\gamma = 2m\omega$, the eigenvalues coincide $\lambda_\pm = -\gamma/2m = -\omega$. However, in this case A is not proportional to the identity, and there is only one linearly independent eigenvector, which can be taken as $(1, -m\omega)^t$. The motion is said to be **critically damped** and the origin is a **degenerate node**. We will look at this case in more detail shortly.

3. If $\gamma > 2m\omega$ (strong damping), then $\lambda_\pm$ are real, distinct and negative ($\lambda_- < \lambda_+ < 0$). The origin is an asymptotically stable node. The motion is said to be **overdamped**: the particle performs less than one full oscillation before coming to rest at $x = 0$.

   In fact, the eigenvectors corresponding to $\lambda_\pm$ can be taken as

   $$\mathbf{w}_\pm = \begin{pmatrix} \lambda_\mp \\ m\omega^2 \end{pmatrix}. \tag{42}$$

   Since $\lambda_- < \lambda_+ < 0$, $\mathbf{w}_+$ points roughly towards west-north-west (WNW) while $\mathbf{w}_-$ points in a NNW direction. They enclose a 'small' wedge in the 2nd quadrant with acute opening angle while $-\mathbf{w}_-$ and $-\mathbf{w}_+$ do so in the 4th quadrant. Similarly, $\mathbf{w}_-$ and $-\mathbf{w}_+$ (or $-\mathbf{w}_-$ and $\mathbf{w}_+$) enclose a 'large' wedge with obtuse opening angle. The trajectory $\mathbf{r}(t) = r_+e^{\lambda_+ t}\mathbf{w}_+ + r_-e^{\lambda_- t}\mathbf{w}_-$ approaches the origin along $\mathbf{w}_+$ as $t \to \infty$. As $t \to -\infty$ both components of $\mathbf{r}$ become unbounded, but the $\mathbf{w}_-$ component grows faster, so $\mathbf{r}$ points along $\pm\mathbf{w}_-$ as $t \to -\infty$. Sketch the phase portrait. We see that x either monotonically approaches 0 or changes sign once (i.e. passes through the equilibrium point once) before eventually reaching 0 as $t \to \infty$. The first case occurs if the IC is in one of the two small wedges with acute opening angles and the latter possibility occurs if the IC lies in one of the two large wedges with obtuse opening angles.

5.2.2 Degenerate eigenvalues and deficient coefficient matrix

The example of the critically damped oscillator encourages us to consider the special case where the two eigenvalues of A are equal but there is only one linearly independent eigenvector. This

degenerate case is somewhat exceptional (non-generic) as a small perturbation of matrix elements would make the eigenvalues distinct. Nevertheless, it is an interesting case as the eigenvectors do not furnish a basis in which to expand a general initial state and the matrix A may be said to be deficient. For instance, consider the 'strictly upper-triangular' system

$$\dot{x} = y, \quad \dot{y} = 0 \quad \text{corresponding to} \quad A = \begin{pmatrix} 0 & 1 \\ 0 & 0 \end{pmatrix}. \tag{43}$$

A has only one eigenvalue 0, with algebraic multiplicity two. The corresponding null-space is spanned by the one linearly independent eigenvector, say $\hat{x} = (1,0)^t$. Thus, the horizontal axis is a line of fixed points. The solution to the IVP is $y = y_0$ and $x = x_0 + y_0 t$. The flow is horizontal and to the right in the upper-half plane and to the left in the lower-half plane. Draw the phase portrait. None of the fixed points is stable, as a small perturbation either upwards or downwards would go off to $x = \pm\infty$.

• More generally, consider the 'upper-triangular' system

$$\dot{x} = \lambda x + y, \quad \dot{y} = \lambda y \quad \text{corresponding to} \quad A = \begin{pmatrix} \lambda & 1 \\ 0 & \lambda \end{pmatrix} \quad \text{with} \quad \lambda < 0. \tag{44}$$

As A is invertible, the origin is the only fixed point. λ is a doubly degenerate eigenvalue with only one linearly independent eigenvector, say $(1,0)^t$, so that the x axis is an invariant subspace with points driven towards the origin: $(x(0),0) \mapsto (x(0)e^{\lambda t}, 0)$. More, generally, since A is upper triangular, y evolves independently of x and is given by $y(t) = y(0)e^{\lambda t}$. We are left with an inhomogeneous equation for x:

$$\dot{x} = \lambda x + y(0)e^{\lambda t} \quad \text{with solution} \quad x(t) = x(0)e^{\lambda t} + y(0)te^{\lambda t}. \tag{45}$$

Draw the corresponding phase portrait noting that the slope of trajectories is given by $y(t)/x(t) = y(0)/(x(0) + y(0)t)$. The slope approaches 0^- in the far past and 0^+ in the far future, so the flow is generally 'clockwise'. The origin is an asymptotically stable degenerate node. In that case, the motion is like that of a critically damped oscillator. The same formulae apply also when $\lambda > 0$, in which case the origin is an **unstable degenerate node**.

• Let us look at the **critically damped oscillator** with $\gamma = 2m\omega$ in more detail

$$\begin{pmatrix} \dot{x} \\ \dot{p} \end{pmatrix} = \begin{pmatrix} 0 & 1/m \\ -k & -2\omega \end{pmatrix} \begin{pmatrix} x \\ p \end{pmatrix}. \tag{46}$$

As noted, the coefficient matrix $A = (0, 1/m| - k, -2\omega)$ has the doubly degenerate eigenvalue $\lambda = -\omega$ with only one linearly independent eigenvector which we take as $\mathbf{w} = (1, -m\omega)^t$. To facilitate solving the equations we will make a similarity transformation to a basis where A is upper/lower triangular (essentially in Jordan form). This basis consists of eigenvectors and generalized eigenvectors of A. Eigenvectors $\mathbf{w}$ are non-trivial solutions to $(A - \lambda I)\mathbf{w} = 0$, they lie in the kernel of $(A - \lambda I)$. Generalized eigenvectors are vectors that lie in the kernel of $(A - \lambda I)^p$ for some $p > 1$ but not in the kernel of $(A - \lambda I)^q$ for $q < p$. In our case $(A - \lambda I)^2$ is identically zero so we can take our generalized eigenvector to be any vector linearly independent of $\mathbf{w}$, say $\mathbf{w}' = (0,1)^t$.

The resulting similarity matrix is $S = (\mathbf{w}, \mathbf{w}') = (1, 0| - m\omega, 1)$ with inverse $S^{-1} = (1, 0|m\omega, 1)$. Applying the similarity transformation we get $J = S^{-1}AS = (-\omega, 1/m|0, -\omega)$

which is upper triangular. The ODE

$$\dot{\mathbf{r}} = A\mathbf{r} = SJS^{-1}\mathbf{r} \quad \text{now becomes} \quad S^{-1}\dot{\mathbf{r}} = J(S^{-1}\mathbf{r}) \quad \text{where} \quad S^{-1}\mathbf{r} = \begin{pmatrix} x \\ m\omega x + p \end{pmatrix}. \tag{47}$$

It is natural to define $y = m\omega x + p$, which evolves independently of x due to the triangular structure:

$$\begin{pmatrix} \dot{x} \\ \dot{y} \end{pmatrix} = \begin{pmatrix} -\omega & 1/m \\ 0 & -\omega \end{pmatrix} \begin{pmatrix} x \\ y \end{pmatrix} \quad \text{or} \quad \dot{y} = -\omega y \quad \text{and} \quad \dot{x} = -\omega x + \frac{y}{m}. \tag{48}$$

Thus

$$y(t) = y_0 e^{-\omega t} \quad \text{and} \quad x(t) = e^{-\omega t}\left(x_0 + \frac{y_0 t}{m}\right) \quad \text{where} \quad y_0 = m\omega x_0 + p_0. \tag{49}$$

The solution to the IVP may now be expressed as

$$x(t) = e^{-\omega t}\left[x_0(1+\omega t) + \frac{p_0 t}{m}\right] \quad \text{and} \quad p(t) = m\dot{x} = e^{-\omega t}\left[-kx_0 t + p_0(1-\omega t)\right]. \tag{50}$$

The origin $(x = 0, p = 0)$ is an asymptotically stable degenerate node. $\mathbf{w}$ is the only invariant subspace. Trajectories that don't start along $\mathbf{w}$ make roughly half a turn clockwise around the origin before reaching it. The phase portrait in the critically damped case may be viewed as resulting from the overdamped portrait when the eigenvectors $\mathbf{w}_\pm$ become collinear and the smaller wedges shrink letting the larger wedges become half-planes. Every trajectory that does not start along $\mathbf{w}$ crosses the equilibrium point $x = 0$ once (at $t = -mx_0/(m\omega x_0 + p_0)$, which may be negative) before eventually reaching the fixed point as $t \to \infty$. Similarly, every (possibly extended) trajectory comes to rest momentarily once at $t = p_0/(kx_0 + \omega p_0)$ before eventually coming to rest at the fixed point.

5.2.3 Trace-determinant classification of fixed points

• While the formulation in terms of eigenvalues allows us, for the most part, to classify fixed points and determine their stability, the (possibly complex) eigenvalues themselves depend only on two real numbers: the trace $\tau = a + d$ and determinant $\Delta = ad - bc$ of $A = (ab|cd)$. Thus, by and large, one obtains a more economical classification in terms of τ and Δ. In other words, though the space of linear systems defined by $A = (ab|cd)$ is four dimensional, the character of the system is largely determined[6] by just two real control parameters τ and Δ. In fact, the characteristic equation for A $(\lambda^2 - \tau\lambda + \Delta = 0)$ implies that the eigenvalues are

$$\lambda_\pm = \frac{1}{2}(\tau \pm \sqrt{\tau^2 - 4\Delta}) \quad \text{with} \quad \tau = \lambda_+ + \lambda_- \quad \text{and} \quad \Delta = \lambda_+\lambda_-. \tag{51}$$

Thus, we may try to determine the nature of the fixed points and phase portrait if we are given a (τ, Δ) pair. To begin with, the sign of the discriminant $D = \tau^2 - 4\Delta$ tells us that $\lambda_\pm$ are (a) distinct and complex conjugates if $D < 0$, (b) real and distinct if $D > 0$ and (c) real and equal if $D = 0$. Evidently, the location of (τ, Δ) relative to the parabola $\Delta = \tau^2/4$ plays a crucial role.

[6] There are exceptional cases where the trace and determinant are not adequate to determine the character of the phase portrait. This happens if A has repeated eigenvalues, as we will see.

At points above the parabola $\Delta > \tau^2/4$, $D < 0$ and the distinct complex conjugate eigenvalues with real part $\tau/2$ imply that there are two main possibilities: (i) (Stable) spiral sink if $\tau < 0$ and (ii) (Unstable) spiral source if $\tau > 0$. We will deal with the boundary $\tau = 0$ below.

At points below the parabola ($\Delta < \tau^2/4$) we have $D > 0$. The eigenvalues are real and distinct and lead to the following main possibilities: (1) saddle if $\Delta < 0$, since in this case the real eigenvalues have opposite signs, (2) unstable node if $\Delta > 0$ and $\tau > 0$ since the eigenvalues are both positive and (3) stable node if $\Delta > 0$ and $\tau < 0$ since the eigenvalues are both negative. Mark these on the $\tau - \Delta$ plane.

We have thus identified five open regions in the $\tau - \Delta$ plane, corresponding to spiral sources and sinks, stable and unstable nodes and finally saddles. A matrix A corresponding to a point in any one such region is generic in the sense that a small change in system parameters a, b, c, d (i.e., while maintaining linearity and reality) does not change the character of the phase portrait.

Special circumstances prevail on the boundaries between the above five regions, with the behavior not always completely determined by the values of τ and Δ. These are the possible borderline cases:

1. **Boundary between spiral sources and sinks:** On the ray $\tau = 0, \Delta > 0$ (symmetry axis of the parabola), the eigenvalues are both imaginary $\lambda_\pm = \pm i\sqrt{|D|}$ and the origin is a center. It is neutrally stable, as befits a system that is borderline between spiral sources and spiral sinks.

2. When $\tau = \Delta = 0$, the eigenvalues vanish and the origin $x = y = 0$ is no longer an isolated fixed point: we may either have a plane of fixed points (if A has two linearly independent eigenvectors so that $A = 0$) or a line of fixed points along the null space of A if A has only one eigenvector (e.g. $A = (01|00)$). The fixed points are neutrally stable in the eigendirection and unstable in any other direction.

3. The parabola $\Delta = \tau^2/4$ lies on the **boundary between spirals and nodes**. On the parabola, the eigenvalues are real and equal $\lambda_\pm = \tau/2$. Let us suppose $\tau, \Delta \neq 0$. If A has two linearly independent eigenvectors, then A is a (non-zero) multiple of the identity and the origin is an unstable star node if $\tau > 0$ and a stable star node if $\tau < 0$. On the other hand, if A is deficient and has only one eigenvector, then the origin is a stable/unstable degenerate node according as τ is negative or positive. This is illustrated by the example $A = (\lambda 1|0\lambda)$ where $\lambda = \tau/2 \neq 0$. Visually, the phase portrait of a degenerate node arises as the phase portrait of a node is morphed to lose one eigenvector. When both eigenvectors cease to be real, the node becomes a spiral.

4. On the other hand, the pair of rays $\Delta = 0, \tau \neq 0$ lie on the **boundary between saddles and nodes**. In this case we have two distinct real eigenvalues $\lambda_- = 0$ and $\lambda_+ = \tau$. We again have a line of fixed points along the null space of A. They are neutrally stable along the null space and unstable/stable in any other direction depending on whether τ is positive or negative.

These borderline cases are of two sorts. Centers lie on the dividing line between spiral sinks and spiral sources. A small change in (τ, Δ) can change the stability of a center. Non-isolated fixed points are similarly on the dividing line between stable/unstable nodes and saddles so that

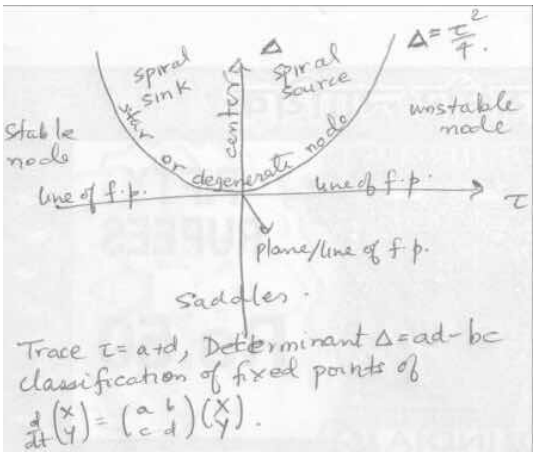

Figure 4: Nature of fixed points on the trace-determinant plane for a 2d linear system.

a small change in (τ, Δ) can alter the stability. By contrast, the stability of symmetrical and degenerate nodes is robust, although they lie on the borderline between nodes and spirals.

In summary, aside from these exceptional cases, we may immediately obtain much information about the phase portrait from the trace and determinant of A. For instance, a negative determinant Δ implies a saddle at the origin, while for positive Δ, we have either a source or a sink according as τ is positive or negative.

We may regard the above regions of the trace-determinant plane as encoding bifurcation diagrams for 2d linear systems. A 1-parameter family of such linear systems would define a curve in the τ-Δ plane. When the curve crosses any of the above boundaries ($\Delta = 0$, $\Delta = \tau^2/4$ and $\tau = 0$ for $\Delta > 0$), the character of the phase portrait changes. For instance, upon crossing the parabola, the origin may go from being a node to a spiral while upon crossing the τ axis, the origin may go from a saddle to a node. In a damped harmonic oscillator, if we increase the damping coefficient γ holding the mass m and frequency ω fixed, the system goes from being underdamped to critically damped at $\gamma = 2m\omega$ and finally overdamped as the number of linearly independent *real* eigenvectors of A goes from zero to one to two. This corresponds to a qualitative change in the phase portrait, with the fixed point at the origin transitioning from a spiral sink to a stable node via a stable degenerate node at the bifurcation point $\gamma = 2m\omega$.

6 Nonlinear vector fields, especially in two dimensions

Given a vector field $\mathbf{v} = (f(\mathbf{r}), g(\mathbf{r}))$ (with $\mathbf{r} = (x, y)$) on the x-y plane, we have the associated IVP

$$\dot{\mathbf{r}} = \mathbf{v}(\mathbf{r}) \quad \text{or} \quad \dot{x} = f(x, y) \quad \text{and} \quad \dot{y} = g(x, y) \quad \text{with} \quad \mathbf{r}(0) = \mathbf{r}_0 = (x_0, y_0). \tag{52}$$

The corresponding trajectory is now a plane curve. As in one dimension, sufficient conditions for existence and uniqueness of solutions are that the components of $\mathbf{v}$ be differentiable with continuous first partial derivatives. If the components f and g are C^1 in some open connected region $R \in \mathbb{R}^2$ containing $\mathbf{r}_0$, then a unique solution to the above IVP exists for some time

$|t| < \tau$. Uniqueness means trajectories cannot cross. This does not prevent two trajectories from approaching each other asymptotically, as they can do at a fixed point.

A special topological feature of dynamics on a plane is that a periodic trajectory (a closed curve) separates the phase plane into an inside and an outside. Trajectories that begin inside cannot wander outside while those that begin outside cannot come in. We will see that the Poincaré Bendixon theorem restricts what they can do. One new possibility that we did not encounter in 2d linear systems is that of a **limit cycle**: an isolated periodic trajectory that is approached asymptotically (as $t \to \infty$ or $-\infty$) by trajectories from the inside and outside. Another new feature is the possibility of **multiple isolated fixed points** and the related possibility of **homoclinic** and **heteroclinic** trajectories. A heteroclinic trajectory approaches a pair of distinct fixed points as $t \to \pm\infty$ while a homoclinic trajectory approaches the same fixed point as $t \to \pm\infty$. Draw examples of phase portraits displaying these.

Though 2d flows arising from autonomous systems are quite interesting and possible to analyze, they do not display chaos, as the trajectories do not have enough room to maneuver. One needs a 3d phase space to find examples of chaos in autonomous systems.

• **Example 1:** As a first example of a nonlinear vector field on the plane, consider Strogatz's system $\dot{x} = x + e^{-y}$ and $\dot{y} = -y$. There is only one fixed point: $(x_* = -1, y_* = 0)$. Since $y(t) = y_0 e^{-t}$ decays to zero, trajectories must asymptotically approach the x axis or lie along the x axis. Thus for large times, $\dot{x} \approx x + 1$ so that $x \approx \text{constant} \times e^t \to \pm\infty$ in the far future, provided we do not begin at the fixed point. This suggests that the fixed point is unstable even though the flow is towards the x axis. This is confirmed by the fact that along the x axis, the solution $x(t) = (x_0 + 1)e^t + 1$ tends to $\pm\infty$ according as x_0 is greater or lesser than -1. In sketching phase portraits, it sometimes helps to draw the **nullclines**. Nullclines are curves along which the flow is either horizontal or vertical. For instance, the flow is horizontal on the nullcline $\dot{y} = -y = 0$, (the x-axis) as already noted. On the other hand, the flow is vertical on the nullcline $\dot{x} = x + e^{-y} = 0$ which corresponds to the graph of the function $y = -\log(-x)$, which lies in the left half-plane. Along this nullcline, the flow is downward for $y > 0$ and upward for $y < 0$. In general, nullclines intersect at the fixed points, in this case there is just one fixed point. What is more, the nullclines divide the phase plane into regions where $\dot{x}$ and $\dot{y}$ have a fixed sign. Here there are four such regions roughly corresponding to the four quadrants. Proceeding from the first quadrant counter-clockwise, the flow is roughly to the south-east, south-west, north-west and north-east. It is important to recognize that nullclines are in general not trajectories[7]. Trajectories can cross nullclines as long as they are not trajectories (in our example, the nullcline $y = 0$ happens to be the union of two trajectories and a fixed point). We may use these facts to sketch the phase portrait, showing that $(-1, 0)$ is a nonlinear version of a saddle. Check the portrait by plotting it numerically using a computer. Having done this, one wonders whether we could have inferred that the phase portrait in the neighborhood of $(-1, 0)$ looks like a saddle with lesser effort. This is indeed possible, by studying the linear approximation to the vector field near the fixed point.

[7] A $\dot{y} = 0$ nullcline is a union of trajectories provided it is horizontal and an $\dot{x} = 0$ nullcline is a union of trajectories if it is vertical

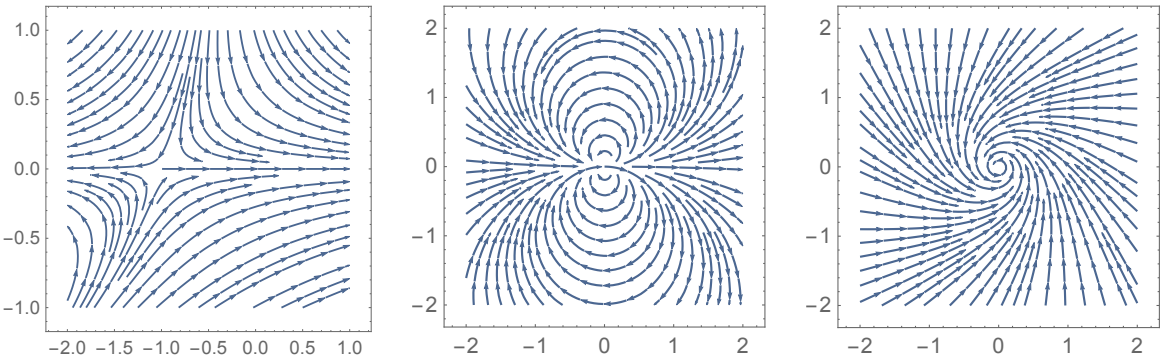

Figure 5: (a) Nonlinear saddle (b) Dipole field mistaken for a plane of fixed points (c) Spiral mistaken for a center.

6.1 Linearization around fixed points

As in 1d, to understand the behavior of a 2d vector field $\mathbf{v}(\mathbf{r}) = (f, g)$ near a fixed point $\mathbf{r}_* = (x_*, y_*)$, it helps to linearize it. Writing $x = x_* + \delta x$ and $y = y_* + \delta y$ for small $(\delta x, \delta y)$, the linearization of the ODEs $\dot{\mathbf{r}} = \mathbf{v}$ reads

$$\frac{d}{dt}\begin{pmatrix}\delta x\\ \delta y\end{pmatrix} = \begin{pmatrix}\frac{\partial f}{\partial x} & \frac{\partial f}{\partial y}\\ \frac{\partial g}{\partial x} & \frac{\partial g}{\partial y}\end{pmatrix}_{\mathbf{r}_*}\begin{pmatrix}\delta x\\ \delta y\end{pmatrix}. \tag{53}$$

The coefficient matrix of this linear system is the Jacobian matrix of first partials, evaluated at the fixed point (indicated by the $\mathbf{r}_*$ subscript).

A natural question is whether we may trust the linearization of $\mathbf{v}$ to correctly capture the qualitative nature of the immediate vicinity of the fixed point. A useful result (more on this in the next section) states that the linearization may be trusted as long as it predicts a fixed point corresponding to a point away from the parabola $\Delta = \tau^2/4$ line $\Delta = 0$ or ray $\tau = 0, \Delta \geq 0$ on the $\tau - \Delta$ plane. In other words, a linear spiral, node or saddle is a spiral, node or saddle of the corresponding nonlinear system (in the sense that the phase portrait of the nonlinear system in a neighborhood of the fixed point can be continuously deformed into that of its linearization). On the other hand, a linear center or non-isolated fixed point *may* or *may not* survive when the effects of nonlinearities are included[8]. Let us consider examples that illustrate some of these features.

• **E.g. 1. A dipole mistaken for a plane of fixed points:** A dipole field is, for instance, the magnetic field around a point magnetic dipole moment on a plane that contains the axis of the dipole. The equations for the field lines (of a dipole at the origin and pointing along x) are given by the system

$$\dot{x} = x^2 - y^2 \quad \text{and} \quad \dot{y} = 2xy. \tag{54}$$

These equations are the real and imaginary parts of $\dot{z} = z^2$ where $z = x + iy$. The origin $(0, 0)$ is the only fixed point. However, the linearization around it leads to a Jacobian matrix that is identically zero. Thus, linear theory would wrongly suggest a plane of fixed points. This happens

[8]Degenerate nodes and star nodes are continuously deformable into ordinary nodes, so the distinction between node, degenerate node and symmetric node is not useful beyond the linear theory.

because the origin is a 'double zero' of the vector field z^2 (similar things happen for vector fields with higher order zeros). The nullclines are the coordinate axes and the lines $y = \pm x$: they intersect that the origin. The flow is upwards on $y = x$ and downwards on $y = -x$. It is to the right on the x-axis and to the left on the y-axis. We can now sketch the phase portrait, which should be familiar from the field lines of an electric or magnetic dipole. In the upper half-plane, all trajectories begin and end at the origin and proceed counter-clockwise: they are homoclinic orbits. The lower half-plane is a mirror image, it consists of clockwise homoclinic orbits. This phase portrait does not resemble that of any linear 2d system: an attempt at a linear approximation does a poor job by producing a plane of fixed points. Homoclinic orbits are an essentially nonlinear phenomenon.

• **E.g. 2. Spiral mistaken for a center:** As noticed in §5.2.3, centers lie on the borderline between spiral sinks and spiral sources. Perhaps not surprisingly, linearization can mistake a spiral for a center. For instance, consider the system $\dot{\theta} = 1$ and $\dot{r} = -ar^n$ in plane polar coordinates $r = (x^2 + y^2)^{1/2} \geq 0$, $\theta = \arctan(y/x)$. For $a = 0$ it is clear that trajectories are concentric circles and we have a (nonlinear) center at the origin. More generally, suppose $a > 0$ and let $n \geq 1$ be an integer. It is clear that r decreases monotonically to zero while θ grows linearly. Hence, the phase point spirals counter-clockwise towards the origin, which is a spiral sink (or source for $a < 0$).

For $n = 1$, the linearized equation $\dot{\delta r} = -a\,\delta r$ has a 1×1 Jacobian with negative eigenvalue and correctly suggests that the origin is a spiral sink for $a > 0$. However, for $n \geq 2$, the linearized equation $\dot{\delta r} = 0$ incorrectly suggests that the origin is a center. Strictly speaking, polar coordinates breakdown at the origin (where θ is not uniquely defined), so to be on the safe side, we should check these conclusions by linearizing the vector field in, say, Cartesian coordinates.

6.1.1 Robustness of the linear (stability) theory and hyperbolic fixed points

Linear centers and non-isolated fixed points of the linearization may not survive when small nonlinear effects are accounted for. However, unlike the neutrally stable center which can be a linear approximation to both a stable and an unstable spiral, the stability of a node (asymmetrical, symmetrical or degenerate) does not change due to nonlinear effects.

If we are only interested in the stability of a fixed point (and are willing to gloss over the difference between, say, a stable degenerate node and a stable node which, in any case, are continuously deformable into each other) then fixed points may be classified into those that have robust (linear) stability and those that are marginal. The robust ones are sinks (attractors), sources ('repellers' or attractors as $t \to -\infty$) and saddles, corresponding to eigenvalues of the linearization that have positive real parts, negative real parts or opposite signs respectively. The stability of such a fixed point is unchanged by nonlinear effects. The marginal ones are centers (with both eigenvalues imaginary) and non-isolated fixed points (where at least one eigenvalue vanishes): their stability can be altered by nonlinear effects. In other words, the marginal cases are those where at least one eigenvalue has zero real part.

• It is useful to introduce a common term for the robust cases: a **hyperbolic fixed point** is one at which all the eigenvalues of the linearization of the vector field have non-zero real parts (this applies to real autonomous systems of dimension one, two or higher). In the above examples, the origin is a hyperbolic fixed point as long as it is an isolated fixed point and not a center.

So saddles, nodes (symmetric or otherwise), spirals and degenerate nodes are all examples of hyperbolic fixed points. The name is a bit misleading: trajectories need not look like hyperbolae in the vicinity of a hyperbolic fixed point (except if it is a saddle)!

The linear approximation faithfully captures the behavior in the neighborhood of a hyperbolic fixed point. The Hartman-Grobman theorem says that the phase portrait in the vicinity of a hyperbolic fixed point is topologically equivalent (or 'conjugate') to that of the linearized system. Topological equivalence means there is a homeomorphism (continuous map with continuous inverse) that maps the local phase portrait (an open neighborhood of the fixed point) to the whole phase plane of the linearized system, taking trajectories to trajectories while preserving the sense of time. Topologically equivalent phase portraits are continuously deformed versions of each other. For instance, a homeomorphism would take fixed points to fixed points, closed orbits to closed orbits and preserve the nature of homoclinic or heteroclinic trajectories.

• Hyperbolic fixed points are structurally stable. This means the topology of the local phase portrait around a hyperbolic fixed point is unchanged by an arbitrarily small perturbation of the vector field. As noted, the phase portrait of a center is not structurally stable: a small perturbation can change the topology of the closed orbits, turning them into spirals. Similarly, a line of fixed points is not structurally stable: a small perturbation can destroy them.

• A feature of hyperbolic fixed points is that for each eigenvalue λ, $e^{\lambda t}$ approaches 0 either as $t \to \infty$ or $-\infty$. By contrast, if the eigenvalue is purely imaginary, then $e^{\lambda t}$ goes round and round the unit circle as $t \to \pm\infty$ and remains at 1 if $\lambda = 0$.

• We can define the stable and unstable manifolds W_s and W_u of a fixed point $\mathbf{r}_*$: the set of points other than $\mathbf{r}_*$ that approach it as $t \to \pm\infty$. For a sink or attractor (e.g. spiral or node), W_u is empty while W_s is the basin of attraction (it includes all points in a sufficiently small open neighborhood of $\mathbf{r}_*$). For a source/repeller W_s is empty while W_u is the 'basin of repulsion' and includes an open neighborhood of $\mathbf{r}_*$.

• What can you say about W_s and W_u for a center?

• Suppose (x_*, y_*) is part of a line/curve (1-parameter family) of fixed points. Give an example of a vector field (with formula and phase portrait) for which the stable and unstable manifolds W_s, W_u of a suitable fixed point (x_*, y_*) are both non-empty. What can you say about W_s and W_u of (x_*, y_*) if the vector field is linear?

• Saddles have non-empty stable as well as unstable manifolds. For a dipole field, W_s and W_u coincide except along the axis of the dipole. Draw phase portraits of suitable vector fields to illustrate these observations.

• **Side remark:** Poincaré developed a discrete time dynamics on the surfaces of section that bear his name. The concepts of stable and unstable manifolds can be extended to the dynamics on a Poincaré surface. He discovered that remarkable things happen when the stable and unstable manifolds of a hyperbolic fixed point intersect transversally (on a Poincaré section through the fixed point). Such a point of intersection is called a homoclinic point (it is not another fixed point). He showed that if there is one homoclinic point, then there is an infinite sequence of them accumulating at the original hyperbolic fixed point. This leads to a very complicated flow pattern which we now associate with chaotic systems. However, this does not happen for autonomous flows in two dimensions. One needs a three or higher dimensional phase space (in which the Poincaré surface is embedded) for homoclinic phenomena and chaos to be possible.

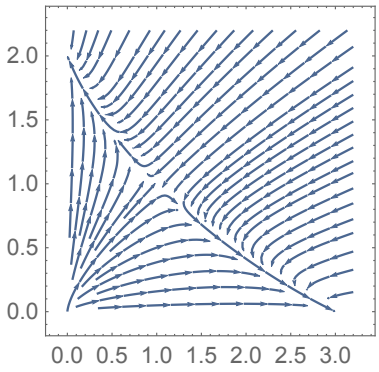

Figure 6: Phase portrait of competitive Lotka-Volterra model. Horizontal and vertical axes are rabbit and sheep populations.

6.1.2 Competitive Lotka-Volterra model

• The competitive Lotka-Volterra equations may be regarded as a generalization of the logistic equation $\dot{N} = rN(1 - N/K)$ for single species population dynamics. It describes competition between two species that share or compete for resources, though neither preys on the other[9]. For example, suppose r and s are the populations of rabbits and sheep (say in 1000s). In suitable units, one postulates that

$$\dot{r} = r(3 - r - 2s) = 3r(1 - r/3) - 2rs \quad \text{and} \quad \dot{s} = s(2 - s - r) = 2s(1 - s/2) - sr. \tag{55}$$

Given that rabbits generally multiply quicker, their linear growth rate (3) is more than that for sheep (2). Left to themselves, the rabbit and sheep populations would approach the respective carrying capacities $K_r = 3$ and $K_s = 2$ reflecting the fact that rabbits require lesser resources. Encounters between rabbits and sheep occur at a rate proportional to the product of the populations and decrease the respective growth rates with the smaller rabbits suffering twice as much. Note that the quadratic terms r^2 and s^2 arise from encounters between members of the same species. Find the fixed points and sketch a phase portrait and discuss its qualitative properties.

Solution: There are four fixed points (r_*, s_*). Three are to be expected from the logistic equation: $(0, 0)$ corresponds to no animals, $(3, 0)$ and $(0, 2)$ correspond to exclusive rabbit or sheep populations equal to their carrying capacities with the other species dying out. Finally, there is a nontrivial fixed point at $(1, 1)$ where rabbits and sheep coexist. To investigate their stabilities, we linearize the system around the fixed points. The Jacobian

$$A = \begin{pmatrix} 3 - 2r - 2s & -2r \\ -s & 2 - r - 2s \end{pmatrix} \tag{56}$$

evaluated at the fixed points is

$$A_{0,0} = \begin{pmatrix} 3 & 0 \\ 0 & 2 \end{pmatrix}, \quad A_{3,0} = \begin{pmatrix} -3 & -6 \\ 0 & -1 \end{pmatrix}, \quad A_{0,2} = \begin{pmatrix} -1 & 0 \\ -2 & -2 \end{pmatrix} \text{ and } \quad A_{1,1} = \begin{pmatrix} -1 & -2 \\ -1 & -1 \end{pmatrix}. \tag{57}$$

Here, the trace and determinant (τ, Δ) are (5,6), (-4,3), (-3,2) and (-2,-1) and are sufficient to characterize the fixed points. (0,0) is an unstable node, (3,0) and (0,2) are stable nodes while (1,1) is a saddle. Since

[9]The model originally introduced by Lotka and Volterra is related but distinct: it deals with predator-prey systems.

all of these are hyperbolic fixed points, the linear theory correctly captures the topological behavior in their vicinity. To get some additional information, we may find the eigenvectors of the Jacobian at the saddle point. The eigenvalues are $\lambda_\pm = -1 \pm \sqrt{2}$ with the corresponding eigenvectors $\mathbf{w}_\pm = a(\mp\sqrt{2}, 1)$ pointing roughly in the West-North-Westerly and ENE directions. $\mathbf{w}_\pm$ are tangent to the unstable and stable manifolds at the saddle $(1, 1)$. Use these facts to qualitatively sketch the phase portrait. There are two heteroclinic trajectories from the saddle: one to each of the single-species nodes. They constitute the unstable manifold of the saddle. Similarly, there is a unique heteroclinic trajectory from the no-animal node (0,0) to the (1,1) saddle point. It forms one part of the stable manifold of the saddle, the other part is a trajectory that comes in from the 'north-eastern' infinity to the saddle point. These two parts of the stable manifold are called separatrices. In fact, they partition the phase portrait $(r, s \geq 0)$ into two regions which are the basins of attraction of the pure sheep and pure rabbit nodes. In conclusion, starting from a generic IC, one of the two species eventually dies out leaving a population of the other species equal to the corresponding carrying capacity. Only the 1-parameter family of ICs that lie on the stable manifold of the saddle point lead to rabbits and sheep coexisting in the far future.

6.2 Conservative systems

Conservative systems are a rather special but important class of autonomous dynamical systems $\dot{\mathbf{r}} = \mathbf{v}(\mathbf{r})$. In essence, they are systems that admit a conserved quantity: a non-trivial dynamical variable that is conserved along the flow (constant on trajectories). Though we will focus on 2d systems, many of the features we discuss generalize to higher dimensions. Newtonian mechanical systems provide interesting examples. Consider Newton's equation for a particle moving in 1d subject to the potential $V(x)$: $m\ddot{x} + V'(x) = 0$. Multiplying by the integrating factor $\dot{x}$ we find that the energy $E = \frac{1}{2}m\dot{x}^2 + V(x)$ is conserved.

More generally, we say that a system $\dot{\mathbf{r}} = \mathbf{v}(\mathbf{r})$ is conservative if it admits a continuous real-valued function $E(\mathbf{r})$ that is not constant on any open subset of phase space and which satisfies $\dot{E} = 0$. A function that is constant on phase space is always trivially conserved, so we must exclude it to ensure that our definition does not classify every dynamical system as conservative!

A simple consequence of the definition is that a conservative system cannot have an attracting or repelling fixed point (such as a node or a spiral). A fixed point $\mathbf{r}_*$ is attracting if all trajectories $\mathbf{r}(t)$ starting from points in a sufficiently small neighborhood approach $\mathbf{r}_*$ as $t \to \infty$. Replacing the condition with $t \to -\infty$ defines a repeller. Now, if a conservative system had an attracting fixed point $\mathbf{r}_*$, then the conserved quantity would be constant throughout its basin of attraction. Since the basin of attraction includes an open set containing $\mathbf{r}_*$, the conserved quantity would be inadmissible. A similar argument applies to repelling fixed points. In the same vein, one may argue that conservative systems cannot admit limit cycles: a limit cycle would imply that the conserved quantity is constant on a narrow ribbon-like open neighborhood of the isolated periodic trajectory. Though spirals and nodes are forbidden, conservative systems can display centers and saddles as well as lines of fixed points.

• **Double-well potential:** The motion of a particle of mass m in a double-well potential $V(x) = (g/4)(x^2 - a^2)^2$ with $g, a > 0$ is governed by Newton's equation $m\ddot{x} = -V'(x) = ga^2x - gx^3$. Putting $p = m\dot{x}$, we get the first order system

$$\dot{x} = p/m \quad \text{and} \quad \dot{p} = ga^2x - gx^3. \tag{58}$$

Find the conserved energy, fixed points, linearization around them, their nature and sketch the phase portrait and indicate any homoclinic orbits.

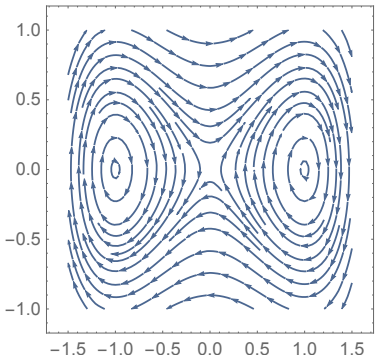

Figure 7: Phase portrait of particle in a double well potential for $m = a = g = 1$.

Solution: The double well potential furnishes an example of a conservative system with saddles and centers. A graph of V shows that there is a potential barrier of height $ga^4/4$ separating two potential wells. There are three fixed points $(x_*, p_*) = (0,0), (a,0)$ and $(-a,0)$. Linearization around these fixed points leads to the Jacobian matrices

$$J_{(0,0)} = \begin{pmatrix} 0 & 1/m \\ ga^2 & 0 \end{pmatrix} \quad \text{and} \quad J_{(\pm a,0)} = \begin{pmatrix} 0 & 1/m \\ -2ga^2 & 0 \end{pmatrix}. \tag{59}$$

While the trace $\tau = 0$ in all cases, the determinant $\Delta_{(0,0)} = -ga^2/m < 0$ while $\Delta_{(\pm a,0)} = 2ga^2/m > 0$. Thus $(0,0)$ is a linear saddle while $(\pm a, 0)$ are linear centers. While the Hartman-Grobman theorem guarantees that the phase portrait in the neighborhood of the origin is homeomorphic to a saddle, it is non-committal on whether the linear centers $(\pm a, 0)$ survive in the nonlinear theory. It turns out that $(\pm a, 0)$ are nonlinear centers: this is a consequence of energy conservation. Since the energy $E = p^2/2m + (g/4)(x^2 - a^2)^2$ is conserved, trajectories must lie along level curves of E. Draw the level curves of E and thereby obtain the phase portrait for the double well potential. Sketch a graph of the energy function over the x-p phase plane showing that it has a bowl-like shape near $(\pm a, 0)$. The energy level contours are the curves along which horizontal planes intersect the graph. One finds that for $E < ga^4/4$, the level contours of energy are a pair of closed curves around $(\pm a, 0)$, so the latter are indeed centers. Physically, they correspond to oscillatory periodic motion around the minima $x = \pm a$ of the potential. As $E \to 0$, the level contours approach a pair of ellipses as is seen by Taylor expanding around $(x = \pm a, p = 0)$:

$$E = \frac{p^2}{2m} + ga^2(x \mp a)^2 + \mathcal{O}(x \mp a)^3. \tag{60}$$

The $E = ga^4/4$ level contour is a figure-8 shaped separatrix that is the union of two homoclinic orbits and the saddle point $(0,0)$. The homoclinic orbits correspond to trajectories where a particle approaches $x = 0$ as $t \to \pm\infty$ from either of the two wells. For $E > ga^4/4$, the level contours of E are 'large' closed curves corresponding to periodic motion that explores both wells. The period of oscillation diverges as $E \to ga^4/4$ either from above or below. The figure-8 shaped separatrix partitions the phase plane into regions where motion is confined/bound to one or other potential well and the region where the particle is unbound/deconfined.

• **Nonlinear centers in conservative systems:** The double-well potential illustrates a general feature of 2d conservative systems $\dot{\mathbf{r}} = \mathbf{v}(\mathbf{r})$. Suppose $\mathbf{r}_*$ is an isolated fixed point of $\mathbf{v}$ that lies at a minimum or maximum of the conserved quantity $E(\mathbf{r})$. Then $\mathbf{r}_*$ is a (nonlinear) center. In other words, all trajectories that start sufficiently close to $\mathbf{r}_*$ are closed and the local phase portrait is homeomorphic to that of a linear center. The reason is that the graph of $E(\mathbf{r})$ over a sufficiently small neighborhood of $\mathbf{r}_*$ must look like a bowl with a unique minimum/maximum

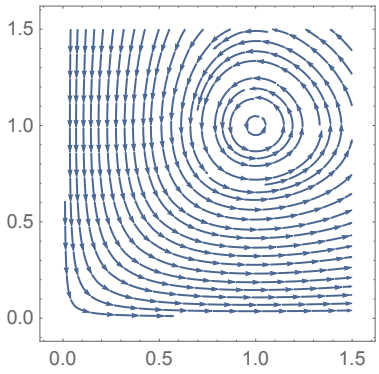

Figure 8: Phase portrait of Lotka-Volterra prey-predator model for $b = p = d = r = 1$. Horizontal and vertical axes are prey and predator populations x and y.

at $\mathbf{r}_*$, whence the energy level contours in the neighborhood must be closed contours. Each such closed level contour must be a trajectory (rather than a union of more than one trajectory) since there cannot be any fixed point at which the trajectory can stop (on account of $\mathbf{r}_*$ being isolated).

6.2.1 Lotka-Volterra prey-predator model

In the model introduced by Lotka (1925) and Volterra (1926), $x(t) \geq 0$ and $y(t) \geq 0$ are the populations of the prey and predator. The per capita growth rates are assumed linear

$$\dot{x} = x(b - py) \quad \text{and} \quad \dot{y} = y(-d + rx) \quad \text{for} \quad b, p, d, r > 0. \tag{61}$$

b and d are the per capita birth and death rates of the prey and predator in the absence of interactions. py and rx are the per capita predation and growth rates of prey and predator due to interspecies interactions. Similar equations are also used to model epidemics, combustion etc.

The system has two fixed points corresponding to extinction $(x_* = 0, y_* = 0)$ and coexistence $(x_* = d/r, y_* = b/p)$. We verify that the Lotka-Volterra system admits a conserved quantity

$$C = d \log x + b \log y - rx - py. \tag{62}$$

The gradient

$$(C_x, C_y) = (d/x - r, b/y - p) \tag{63}$$

vanishes precisely at the above two fixed points. The Hessian of C is the diagonal matrix $\mathrm{diag}(-d/x^2, -b/y^2)$ and evaluates to $\mathrm{diag}(-r^2/d, -p^2/b)$ at the coexistence fixed point. The latter is therefore a local maximum of C and is therefore a center. Trajectories lie along level contours of C in the 1st quadrant of the x-y (prey-predator) plane (see Fig. 8). These level contours are closed curves encircling the center at the coexistence fixed point. Thus, generically, the populations are periodic and oscillate in 'cycles' around the coexistence values.

6.3 Hamiltonian systems

• Hamiltonian systems are a physically important class of conservative systems. The simplest possibility is a Hamiltonian system on the phase plane with canonical coordinates x and p,

usually representing position and momentum of a particle. The system is defined by a distinguished real-valued (and sufficiently smooth) function $H(x,p)$ called the Hamiltonian, that is not constant on any open subset of the phase space. The Hamiltonian generates the flow via Hamilton's equations

$$\dot{x} = \frac{\partial H}{\partial p} \quad \text{and} \quad \dot{p} = -\frac{\partial H}{\partial x}. \tag{64}$$

The difference in sign between the two equations and the switch between x and p are essential and distinguish Hamiltonian flows from gradient flows $(\dot{x},\dot{y}) = -(\partial_x f, \partial_y f)$. Unlike gradient flows where f is non-increasing along trajectories, H is conserved in Hamiltonian systems. Indeed,

$$\dot{H} = \frac{\partial H}{\partial x}\dot{x} + \frac{\partial H}{\partial p}\dot{p} = \frac{\partial H}{\partial x}\frac{\partial H}{\partial p} - \frac{\partial H}{\partial p}\frac{\partial H}{\partial x} = 0. \tag{65}$$

The Hamiltonian vector field $V_H = (\partial_p H, -\partial_x H)$ is said to be the skew gradient of H. The transformation of the phase space generated by a Hamiltonian flow is an example of a canonical transformation (other canonical transformations that are continuously connected to the identity transformation arise by picking other Hamiltonian functions).

• Somewhat more generally, we may define a Hamiltonian system on a 2d phase space (surface M that is not necessarily a plane) if we are given a smooth real-valued Hamiltonian function H and a non-degenerate (invertible) second rank antisymmetric tensor field r^{ab} on it. If ξ^1, ξ^2 are local coordinates on M, then Hamilton's equations are

$$\dot{\xi}^a = r^{ab}\frac{\partial H}{\partial \xi^b} = (\omega^{-1})^{ab}\frac{\partial H}{\partial \xi^b}. \tag{66}$$

Verify that these equations reduce to Hamilton's canonical equations on the phase plane if $(\xi^1,\xi^2) = (x,p)$ and $r^{ab} = (0,1|-1,0)$. The skew-symmetric tensor r^{ab} is called the Poisson tensor and its inverse $\omega = r^{-1}$ $(\omega_{ab}r^{bc} = \delta_a^c)$ is called the symplectic form. The Hamiltonian vector field $V_H^a = r^{ab}\partial_b H$ is the symplectic gradient of the Hamiltonian.

• Harmonic and anharmonic oscillators, particle motion in a double well potential, motion of a simple pendulum or Euler top are some examples of Hamiltonian systems.

• **Remark:** It is possible to generalize the concept of Hamiltonian dynamical systems to phase spaces (symplectic manifolds (M,ω)) of any even dimension ≥ 2. The above formula for the Hamiltonian vector field is unchanged, but one additionally requires that the symplectic 2-form be closed $d\omega = 0$. Even more generally, one may define Hamiltonian flows $(\dot{\xi}^a = r^{ab}\partial_b H)$ on Poisson manifolds (M,r) of any dimension ≥ 2 by requiring that the Poisson tensor r^{ab} satisfy a quadratic relation called the Jacobi identity.

6.3.1 Some general properties of Hamiltonian systems

Lack of nodes, spirals and limit cycles: Since Hamiltonian systems are conservative, it follows that they do not admit attractive or repulsive fixed points (nodes or spirals) or limit cycles.

Liouville property: In fact, Hamiltonian systems have a much stronger property, the Liouville property of preservation of phase space area (or volume in higher dimensions) under the flow. In the simplest case of canonical coordinates, the area element on the phase plane is defined as $dx \wedge dp$. Liouville's theorem says that this area element is preserved by the flow, so that the

area of any region is unchanged as it moves under the flow. To see that $dx \wedge dp$ is preserved, we consider the infinitesimal canonical transformation generated by a Hamiltonian flow over a small time ϵ treated to linear order:

$$x' = x + \epsilon \partial_p H + \mathcal{O}(\epsilon^2), \quad \text{and} \quad p' = p - \epsilon \partial_x H + \mathcal{O}(\epsilon^2). \tag{67}$$

From multivariable calculus, the transformed area element is given by

$$dx' \wedge dp' = (\det J) dx \wedge dp \quad \text{where} \quad J = \begin{pmatrix} \partial_x x' & \partial_p x' \\ \partial_x p' & \partial_p p' \end{pmatrix} \approx \begin{pmatrix} 1 + \epsilon H_{px} & \epsilon H_{pp} \\ -\epsilon H_{xx} & 1 - \epsilon H_{xp} \end{pmatrix} \tag{68}$$

and $H_{xp} = \partial_p \partial_x H$ etc. On account of the equality of mixed partials, $\det J \approx 1 + \epsilon^2 (H_{xx} H_{pp} - H_{xp}^2)$. Thus, to order ϵ, there is no change in the area element under Hamiltonian evolution.

• **Remark:** On a symplectic surface, the area element is given by the symplectic two-form $\omega = \frac{1}{2} \omega_{ab} d\xi^a \wedge d\xi^b$. One can show that ω is Lie-dragged by the Hamiltonian vector field $\mathcal{L}_{V_H} \omega = 0$. More generally, on a $2n$-dimensional symplectic manifold, one defines the volume element as the n^{th} exterior power ω^n of the symplectic form. One shows that $\mathcal{L}_{V_H} \omega = 0$ which implies (by the Leibniz rule) that $\mathcal{L}_{V_H} \omega^n = 0$, so that phase space volume is preserved by a Hamiltonian flow.

• The Liouville property rules out nodes, spirals and limit cycles in Hamiltonian systems: the flow around an attractive or repulsive fixed point or limit cycle cannot preserve phase space volume as the entire basin of attraction/repulsion (with non-zero area) is mapped by the flow (as $t \to \infty$ or $-\infty$) to a single point or a closed curve (having zero area or volume).

• While spirals and nodes are ruled out, planar Hamiltonian systems can have saddles and centers, as the dynamics in a double well potential shows. What is the nature of the linearization of the Hamiltonian vector field around a fixed point?

6.3.2 Poincaré recurrence

Recurrence is a generalization of periodic behavior where one gives up exact return to the initial state for approximate return to the initial state to any prescribed accuracy. We ask for conditions that will guarantee that a trajectory will eventually return to a prescribed neighborhood of an initial phase point and ask how many times it will return to that neighborhood. Let us begin with examples that illustrate some of the possibilities.

• **E.g. 1: Linear harmonic oscillator:** Here $H = (1/2)(p^2 + \omega^2 x^2)$ and we have a center at the origin. Every non-constant trajectory is periodic with period $2\pi/\omega$. Thus the system is recurrent. We notice that this happens even though the phase space has infinite volume.

• **E.g. 2: The double well potential:** corresponds to $H = p^2 + g(x^2 - a^2)^2$ and has a saddle at the origin along with a pair of centers at $(\pm a, 0)$. All trajectories other than the two homoclinic ones are periodic. However, the period varies with energy and diverges as we approach the separatrix at $E = ga^4$ from above or below. Thus all trajectories other than those that begin on the homoclinic orbits return to the initial state, and the system is recurrent, though with a recurrence time that varies with location on phase space.

• **E.g. 3: Irrational windings on a torus:** Not all Hamiltonian systems need have fixed points or periodic trajectories. Consider flow on a 2-torus with 2π-periodic coordinates θ_1 and

θ_2. We can view the phase space as the square $0 \leq \theta_{1,2} \leq 2\pi$ with the opposite edges identified. The evolution is defined by the the equations

$$\dot{\theta}_1 = \omega_1 \quad \text{and} \quad \dot{\theta}_2 = \omega_2 \quad \text{where} \quad (\omega_1, \omega_2) \neq (0,0). \tag{69}$$

Since the frequencies are not both zero, the system does not possess any fixed points. The trajectories are straight lines on the square:

$$\theta_1 = \omega_1 t + \theta_1(0) \quad \text{and} \quad \theta_2 = \omega_2 t + \theta_2(0). \tag{70}$$

When a trajectory reaches an edge of the square (say at $(\theta_1 = 2\pi, \theta_2)$), it continues from the opposite edge (say $(\theta_1 = 0, \theta_2)$) with the same slope and direction. So a trajectory on the phase square typically looks like a collection of oblique parallel lines with slope ω_2/ω_1. It is clear that the evolution preserves the area on the phase space measured with respect to the element $d\theta_1 \wedge d\theta_2$. In fact, if we postulate that θ_1 and θ_2 are canonically conjugate $\{\theta_1, \theta_2\} = 1$ we may derive the equations of motion (locally[10]) from the linear Hamiltonian $H = -\omega_2\theta_1 + \omega_1\theta_2$

$$\dot{\theta}_1 = \{\theta_1, H\} = \omega_1 \quad \text{and} \quad \dot{\theta}_2 = \{\theta_2, H\} = \omega_2. \tag{71}$$

Now both θ_1 and θ_2 evolve periodically in time, with periods $T_1 = 2\pi/\omega_1$ and $T_2 = 2\pi/\omega_2$. However, the superposition of these two periodic motions need not be periodic. If $T_1 = 2T_2$ then the phase trajectory is periodic with period T_1. More generally, if T_1 and T_2 are commensurate (i.e., if there exist integers $m, n \neq 0$ such that $mT_1 + nT_2 = 0$), then the periods have a 'least common multiple' (LCM) and the trajectory is periodic (it is a closed curve on the torus). On the other hand, if they are incommensurate (T_2/T_1 or T_1/T_2 is irrational), then the trajectory is not closed: it is as if the LCM has gone to infinity, the trajectory is aperiodic and keeps winding around the torus without ever returning to the initial state. In fact, one can show that for incommensurate frequencies, every trajectory is aperiodic and fills up the torus, in the sense that it comes arbitrarily close to any given point on the torus. Thus, irrational windings on a torus provide an example of a Hamiltonian system that displays recurrent motions without admitting any periodic trajectories.

• **E.g. 3: Free particle and Kepler problem.** Not all Hamiltonian systems display recurrence. In fact, free particle motion on a line is not recurrent in general. If it has non-zero initial momentum, the particle goes off to infinity without ever returning to a given neighborhood of the initial location: $x(t) = x(0) + p(0)t/m \to \pm\infty$ depending on the sign of $p(0)$. Similarly, dynamics in the Kepler problem $H = (1/2)\mathbf{p}^2 - GMm/|\mathbf{r}|$ is not recurrent. Trajectories with $H < 0$ are periodic, corresponding to elliptical orbits in configuration (position) space while trajectories with $H > 0$ fly off to infinity along hyperbolic orbits. These two examples indicate that having a phase space of infinite volume without any force to contain the motion to a region of finite volume could come in the way of recurrence.

The Poincaré recurrence theorem applies to a Hamiltonian system with a phase space of any dimension but having a finite phase volume (measured with respect to the Liouville volume element)[11]. The theorem says that given any open set N_0 of initial conditions of positive volume

[10] Note that this Hamiltonian is not globally well-defined on the torus: it is multi-valued.

[11] These are simple sufficient conditions, they can sometimes be relaxed without losing recurrence, as the examples of the harmonic oscillator and double-well potential indicate. The recurrence theorem was conjectured by H. Poincaré in 1890 and proved by C. Carathéodory in 1919.

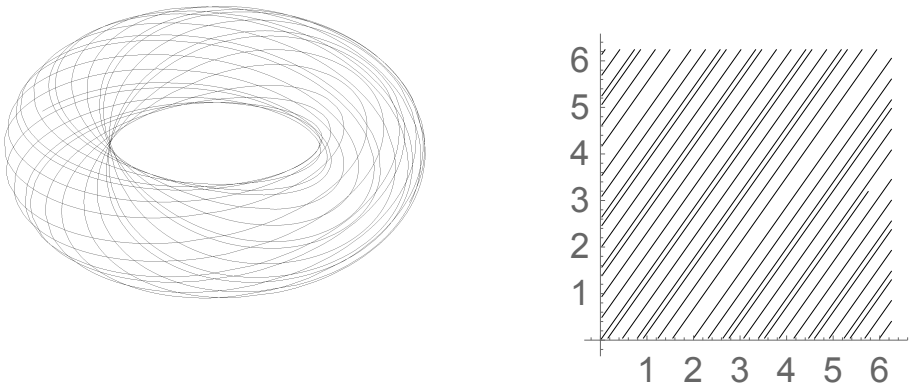

Figure 9: Left: Irrational windings on a torus: $\theta = \omega_1 t$ and $\phi = \omega_2 t$ for $0 \leq t \leq 100$ with $\omega_1 = 1, \omega_2 = \sqrt{2}$. The embedding used is $x = R + r\cos\theta\cos\phi$, $y = R + r\cos\theta\sin\phi$ and $z = r\sin\theta$ with $r = 1$ and $R = 3$. Right: $(\theta(t), \phi(t))$ plotted modulo 2π on a square with periodic boundary conditions.

in phase space, almost every trajectory that begins in it (with the possible exception of those beginning from a subset of zero volume) returns to N_0, and does so infinitely often.

Sketch of the proof: The proof exploits the Liouville property of preservation of phase volume as well as the assumption of finite phase volume. Suppose we consider ICs lying in an open set N_0 (say an open ball) with necessarily non-zero volume. After a time t, Hamiltonian evolution takes N_0 to a region N_t with the same volume. Now, the family of phase trajectories starting in N_0 trace out a tubular region in phase space whose volume must be an increasing (non-decreasing) function of time. *Step 1*: One possibility is that N_t always intersects N_0 in a set of non-zero volume $\cap_{t\geq 0} N_t$. In this case, all trajectories in this intersection remain within it and the assertion of the theorem is true for this set, and we may proceed to *Step 2*. On the other hand, suppose there is a first time at which the volume of $N_t \cap N_0$ drops to zero. In this case, we will argue that there must be a later time t_1 after which N_t and N_0 intersect in a region of non-zero volume. This is because the volume of the phase tube is increasing but cannot exceed the total volume of the phase space. Thus, there must come a time when the phase tube 'intersects itself'. The first such intersection must be of N_{t_1} with N_0 rather than with any $N_{t'>0}$ since all points of $N_{t'}$ evolved back in time start from N_0. Thus, after a time t_1, N_{t_1} and N_0 must intersect in a set of non-zero volume. Thus, trajectories starting from a non-zero fraction of the volume of N_0 return to N_0 after t_1. *Step 2:* We now apply the same argument to the remaining portion of N_0 (i.e., interior of $N_0 \setminus N_{t_1}$) to conclude that there is a time t_2 after which trajectories starting from a non-zero fraction of the volume of $N_0 \setminus N_{t_1}$ return to it. Proceeding in this manner, one argues that except possibly for a subset of zero volume, every trajectory starting in N_0 returns to N_0. *Step 3:* Now we repeat the whole argument to show that almost every trajectory that begins in N_0 returns to N_0 twice and so on, thus establishing the theorem.

• **Remarks:** (a) Note that the time at which the trajectory returns to N_0 for the second time need not be twice the time of first return. Moreover, the recurrence times tend to grow as the volume of N_0 is decreased (this is easily seen for irrational windings on a torus). (b) There can be initial conditions in N_0 that never return to N_0: an example is provided by ICs that lie on

homoclinic orbits in the double well potential problem. (c) There can be exceptional ICs and sets N_0 for which a trajectory returns to N_0 a finite number of times, and then stops doing so.

6.4 Index theory

• The index of a vector field around a closed curve C measures how much the vector field rotates as one goes around C. In contrast with the linearization, which typically provides local information around a fixed point, the index can provide global information on the phase portrait. It is an integer that contains information on the fixed points that may lie inside C. We may view C as a probe used to extract information about the vector field, just as a Gaussian surface or Amèprian loop are probes used to determine the charge or current enclosed in electrostatics and magnetostatics.

• Suppose C is a (counter-clockwise directed) simple closed curve (no self-intersections and no retracing) that does not pass through any fixed points of the 2d vector field $\mathbf{v}$. Note that C need not be a trajectory. Then, at each point of C, the angle ϕ (measured counter-clockwise) that $\mathbf{v}$ makes with the horizontal x-axis is defined. Now ϕ changes continuously as we traverse the curve. The index I_C is defined as the net change in ϕ (in units of 2π) as we go counter-clockwise round C once.

• More precisely, suppose $\mathbf{v} = (f, g)$ and let C be the curve $\mathbf{r}(s) = (x(s), y(s))$ parameterized by $0 \leq s \leq 2\pi$. Then the angle $\mathbf{v}(\mathbf{r}(s))$ makes with the horizontal is $\phi(s) = \arctan(g(\mathbf{r}(s))/f(\mathbf{r}(s)))$. The infinitesimal change in ϕ as s is incremented by ds is

$$d\phi = \frac{d\phi}{ds} ds = \frac{f\frac{dg}{ds} - g\frac{df}{ds}}{f^2 + g^2}\, ds. \tag{72}$$

Here f and g depend on s through x and y, so with subscripts denoting partial derivatives,

$$\frac{dg}{ds} = g_x x'(s) + g_y y'(s) \quad \text{and} \quad \frac{df}{ds} = f_x x'(s) + f_y y'(s). \tag{73}$$

Note that $x'(s)$ and $y'(s)$ are not to be confused with the velocities $\dot{x}(t)$ and $\dot{y}(t)$ which are defined only along a trajectory. Thus, the change in ϕ upon going around the contour C is

$$I_C = \frac{1}{2\pi} \oint d\phi = \frac{1}{2\pi} \int_0^{2\pi} \frac{f g_s - g f_s}{f^2 + g^2}\, ds. \tag{74}$$

Since $\mathbf{v}$ returns to its original direction after one trip around C, the change in ϕ must be a multiple of 2π, whence I_c must be an integer. I_c counts the number of counter-clockwise revolutions that the vector field makes during one circuit around C.

• The index only depends on the vector field on C and not inside or outside C. We may think of the above formula as an analogue of the LHS in Gauss' law in electrostatics

$$\int_{\text{closed surface}} \mathbf{E} \cdot \hat{n}\, dS = \frac{Q_{\text{encl}}}{\epsilon_0}. \tag{75}$$

We wish to find the analogue of the RHS. What plays the role of charge enclosed? Let us now compute the index in some examples to gain some intuition.

• In simple cases, one can **find the index pictorially** by following how the vector field rotates as one traverses C once counterclockwise. One simply draws arrows on C at a few reasonably

spaced points showing the direction of $\mathbf{v}$ and counts how many full turns it makes. Try this out for the examples that follow.

• **E.g. 1: Constant vector field:** A constant vector field, say, $\mathbf{v} = (f = 1, g = 0)$ doesn't have any fixed points. f_s and g_s both vanish, so the index of any closed curve vanishes. We could have obtained this result pictorially by drawing the vector field along the curve and observing that $\mathbf{v}$ does not change direction as we go around C. It is plausible that the index continues to vanish even if the vector field is not constant but fluctuates a little bit in direction without 'turning around'.

• **E.g. 2: C encloses a node:** The linear system $\dot{x} = ax$ and $\dot{y} = ay$ has a symmetrical node at the origin for any $a \neq 0$. We take C to be the unit circle centered at the origin and traversed counter-clockwise ($x = \cos s, y = \sin s$) for $0 \leq s \leq 2\pi$. Thus

$$g_s = g_y y_s = a \cos s = ax \quad \text{and} \quad f_s = f_x x_s = -a \sin s = -ay. \tag{76}$$

Thus

$$\frac{d\phi}{ds} = \frac{(f g_s - g f_s)}{f^2 + g^2} = \frac{xx - y(-y)}{x^2 + y^2} = 1 \quad \text{and} \quad I_C = \frac{1}{2\pi} \int_0^{2\pi} ds = 1. \tag{77}$$

Notice that $I_C = 1$ both for positive and negative a (source and sink inside C).

• Argue pictorially that $I_C = 1$ for a vector field that points roughly radially outwards or inwards along a closed curve that is roughly a circle enclosing the origin.

• **E.g. 3: C encloses a saddle point:** Suppose $\dot{x} = f = x$ and $\dot{y} = g = -y$ and C is the counter-clockwise unit circle $(x, y) = (\cos s, \sin s)$ enclosing the saddle at the origin. Then it is easily checked that

$$\frac{d\phi}{ds} = \frac{-x y_s + y x_s}{x^2 + y^2} = -1 \quad \Rightarrow \quad I_C = -1. \tag{78}$$

• **E.g. 4: C is a circular trajectory around a center:** Consider the linear oscillator with $m = k = \omega = 1$: $\dot{x} = f = p$ and $\dot{p} = g = -x$, whose trajectories are clockwise directed concentric circles around the center at the origin. Choose C to be the unit circle $(x, y) = (\cos s, \sin s)$ (we could even take $s = -t$). Proceeding as before, we find $I_C = 1$.

• **E.g. 5: C is a circular contour around a spiral:** Consider the under-damped oscillator

$$\dot{x} = p/m \quad \text{and} \quad \dot{p} = -kx - (\gamma/m)p \quad \text{with} \quad \gamma < 2m\omega, \tag{79}$$

which has a spiral sink at $x = p = 0$. Show that $I_C = 1$ for C a unit circle. Check that the index does not change if we make the spiral sink into a source. This can be achieved by rotating the vector field at each point by π, however, this will not change the net change in angle ϕ.

6.4.1 Properties of the index

• The above examples have prepared us for the following properties of the index.

• If the closed contour C' may be obtained from C by **continuous deformation** without passing through any fixed points, then $I_C = I_{C'}$. To see this, we first note that the index I_C must vary continuously as C is deformed. Since I_C is a continuous integer-valued function of C, it must be a constant.

• The index of a closed **curve that does not enclose any fixed points** is zero. This is because we may continuously shrink C without changing I_C and without encountering any fixed points till C is just a point and $I_C = 0$. Alternatively, once C is sufficiently small, the vector field is approximately a constant field over it, so $I_C = 0$ as in Example 1.

• **The index I_C is additive under sub-division of the contour.** Suppose C is a circle and we draw a diameter (that does not pass through a fixed point), thereby defining two D-shaped simple closed contours C_1 and C_2 whose concatenation is C. C_1 and C_2 traverse the common diameter in opposite directions so that it does not contribute to the index. Thus we see that $I_C = I_{C_1} + I_{C_2}$. This holds more generally when C is the concatenation of C_1 and C_2

• The index I_C is unchanged if we reverse the direction of the vector field everywhere, i.e., $\mathbf{v} \to -\mathbf{v}$ or $(f, g) \to (-f, -g)$ or $t \to -t$. It is clear that I_C does not change since $d\phi = (fg_g - gf_s)/(f^2 + g^2)$ is unchanged. This explains why the index of the curve in E.g. 2 was independent of the sign of a (i.e., whether C enclosed a stable or unstable node).

• More generally, if we rotate the vector field at every point of the phase plane by the same angle ϕ_0, then all the angles ϕ are augmented by ϕ_0 so that the index of any given curve is unchanged.

• If C is a **closed orbit**, then $I_C = 1$. We found that this is the case for a trajectory of the linear harmonic oscillator. A sketch makes this plausible for any closed trajectory: the vector field rotates once counter-clockwise as we follow it once counter-clockwise around a trajectory. Note that by convention, we take C to run counter-clockwise irrespective of the sense of the trajectory.

• **Index of a point:** We may use the invariance of I_C under continuous deformation of C to define the index of an isolated fixed point or regular point. Suppose $\mathbf{r}_*$ is an isolated fixed point, then we define its index $I_{\mathbf{r}_*}$ to be I_C for *any* counter-clockwise closed curve C that encloses $\mathbf{r}_*$ and no other fixed point. On the other hand, if $\mathbf{r}$ is a regular point, i.e., not a fixed point and with no fixed point in any sufficiently small neighborhood, then we define its index $I_{\mathbf{r}}$ to be I_C for any counterclockwise curve C that encloses $\mathbf{r}$ and no fixed point. It is clear that the index of a regular point vanishes.

• Since the local phase portrait of a nonlinear node/spiral or saddle is homeomorphic to that of a linear node/spiral or saddle, our examples show that $I_{\text{node}} = I_{\text{spiral}} = +1$ while $I_{\text{saddle}} = -1$. Unfortunately, the index cannot be used to distinguish between a node and a spiral. On the trace-determinant $(\tau - \Delta)$ plane classifying linear systems, we observe that the index is $+1$ for $\Delta > 0$ and -1 for $\Delta < 0$. Evidently, the index is not directly related to stability but changes discontinuously as we cross the τ-axis. The notion of the index of a fixed point allows us to arrive at a simple expression for the index of a closed curve.

• **Index of C as the sum of indices of enclosed fixed points.** Suppose C is a simple closed curve that encloses n isolated fixed points $\mathbf{r}_{1*}, \mathbf{r}_{2*}, \ldots, \mathbf{r}_{n*}$ with indices $I_{\mathbf{r}_{1*}}, \ldots, I_{\mathbf{r}_{n*}}$. Then the index of C is the sum of the indices of the enclosed fixed points. **Exercise:** Sketch the proof.

Answer: The idea of the proof is to continuously deform C (with out changing I_C) so that it consists of small nearly closed curves C_j surrounding each of the fixed points $\mathbf{r}_j$ and narrow 'two-way' paths connecting adjacent C_js. Draw a picture. In the limit of infinitesimally narrow bridges, their contribution to I_C cancels out when accounting for the upstream and downstream portions, while $I_{C_j} \to I_{\mathbf{r}_{j*}}$. Thus

we obtain

$$I_C = I_{\mathbf{r}_{1*}} + I_{\mathbf{r}_{2*}} + \cdots + I_{\mathbf{r}_{n*}}. \tag{80}$$

• **Corollary:** An immediate consequence is that a closed trajectory must enclose at least one fixed point, since the index of a closed trajectory is 1. For instance, a closed trajectory can enclose a single spiral or node but cannot enclose a single saddle or two nodes and no other fixed points. In favorable cases, we may use this result along with a knowledge of the locations of fixed points and their indices to rule out closed trajectories. Show that the competitive Lotka-Volterra model cannot have any periodic solutions.

• **There are examples of fixed points with any integer index.** For example, the fixed point at the origin for the dipole field $\dot{x} = x^2 - y^2$, $\dot{y} = 2xy$ has index 2. Show this by sketching the vector field and choosing C to be a unit circle centered at the origin.

• **A fixed point can have index zero.** An example is furnished by the fixed point at the origin for the vector field $\dot{x} = x^2$ and $\dot{y} = y^2$. The vector field fluctuates between pointing to the north and to the east without ever rotating. One checks that the index of any closed curve enclosing the origin vanishes. Thus, regular points are not the only ones with index zero.

• **Index as degree:** The index can be regarded as the degree of a map between circles. Consider a planar vector filed. Let $C(s) : [0, 2\pi] \to \mathbb{R}^2$ be a simple closed curve as before, it is homeomorphic to a circle. At each point of C consider the normalized vector field $\hat{n}(s) = \mathbf{v}(s)/|\mathbf{v}(s)|$, which is a unit vector, so it lies on a circle. As we go round C once we follow the movement of $\hat{n}(s)$ around the unit circle: it must return to its starting point as $\hat{n}(0) = \hat{n}(2\pi)$. Thus we get a map from $S^1 \to S^1$ taking $s \mapsto \hat{n}(s)$. This map could be many-to-one and the number of times the curve C covers the target circle is called its degree. If the vector field is a constant, then $\hat{n}(s) \equiv \hat{n}(0)$ does not move and the degree is zero. If $\hat{n}$ goes once round the circle counterclockwise (or clockwise) we say that the map has degree +1 (or -1). Note that $\hat{n}(s)$ can go back and forth, it may retrace its path sometimes. More generally, the map may be a double cover, triple cover or n-fold cover. The index, defined as the degree of this map, allows us to generalize the index to vector fields on curved surfaces. For a surface M embedded in 3d Euclidean space, $\hat{n}$ must lie on a 2-sphere and trace out a curve which is an n-fold cover of a circle.

• **Index of vector fields on Riemann surfaces:** Consider a smooth vector field on a compact (closed, bounded) surface without boundaries. Examples include the sphere, torus and higher handlebodies. These 'Riemann' surfaces are classified by their genus, a non-negative integer which is the number of handles: $g = 0$ for the sphere, $g = 1$ for the torus, $g = 2$ for the double torus etc. The Poincaré-Hopf index theorem states that for a smooth vector field on a surface of genus g, the sum of indices of the fixed points of a vector field is equal to the Euler characteristic $\chi = 2 - 2g$. In particular, every such vector field on a sphere ($\chi = 2$) has to have at least one fixed point: there is no nonvanishing vector field on the sphere – this is sometimes called the hairy ball theorem and says that one cannot consistently comb hair (of non-zero length) tangentially everywhere on a sphere. On the other hand, one can imagine a vector field on the sphere whose integral curves point longitudinally, emerging from a node at the north pole and ending up at a node at the south pole (the poles each have index one). Another example is a vector field with integral curves that are latitudes: it has two fixed points, centers at the poles. On a torus, $\chi = 0$, so the torus admits vector fields that are nowhere vanishing; for instance one that points azimuthally everywhere.

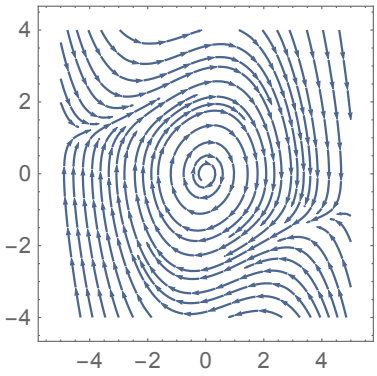

Figure 10: Limit cycle of the van der Pol oscillator for $m = k = 1$ and $\mu = 1/5$. Notice the unstable spiral at the origin.

6.5 Limit cycles

As noted earlier, a limit cycle is an isolated periodic orbit. Though a limit cycle can exist in a phase space of any dimension $d \geq 2$, we will confine our discussion to two dimensions. In the case of a plane, the limit cycle partitions the phase space into an inside and an outside. Since a limit cycle is isolated, trajectories that begin in a sufficiently small tubular neighborhood cannot be periodic and must spiral either toward or away from the limit cycle. This leads to stable, unstable and half-stable limit cycles.

Linear systems do not admit limit cycles, since a slightly rescaled periodic orbit ($\lambda \mathbf{r}(t)$ for $\lambda \approx 1$) must also be a periodic orbit of the linear system, so that $\mathbf{r}(t)$ cannot be isolated.

Stable limit cycles, when they exist, represent dynamically generated (self-sustained, i.e., without external periodic driving) oscillations of a nonlinear system with a dynamically determined asymptotic ($t \to \infty$) period and waveform, including amplitude. By contrast, periodic trajectories of a linear system can have any amplitude by a suitable choice of ICs, due to the freedom to rescale a periodic trajectory. There are several examples of periodic motions that may be modeled as limit cycles: airplane wing flutter, vibrations in bridges, oscillations in populations in predator-prey systems, the heart beat, daily rhythms in body temperature and sleep, hormone secretion etc.

E.g. 1: Limit circle in plane polar coordinates: It is easy to cook-up a limit cycle in a nonlinear system on the plane using polar coordinates. In fact, consider the system

$$\dot{r} = r(1 - r) \quad \text{and} \quad \dot{\theta} = 1. \tag{81}$$

The angular motion is uniform counterclockwise rotation and decouples from the radial motion which has a repulsive fixed point at $r = 0$ and an attractive one at $r = 1$. Thus, the circle $r = 1$ is a stable limit cycle with trajectories spiraling towards it from either side. The limit cycle is the circular orbit $(x, y) = (\cos t, \sin t)$.

E.g. 2: van der Pol oscillator: A more non-trivial example of a limit cycle arises in the van der Pol equation:

$$m\ddot{x} = -kx - \mu(x^2 - 1)\dot{x} \quad \text{for} \quad m, k, \mu > 0. \tag{82}$$

The vdP equation arose (when van der Pol was working with vacuum tubes at Philips in the

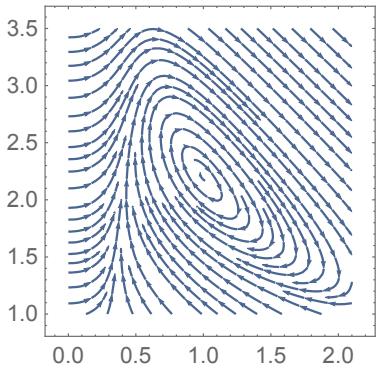

Figure 11: Limit cycle of the Brusselator for $a = 1$ and $b = 2.2 > 1 + a^2$ where the fixed point at $(a, b/a)$ is a spiral source.

Netherlands) in modeling LCR electrical circuits where the 'resistor' had a nonlinear V-I characteristic making it behave like a resistor (sink) for currents of large magnitude and an anti-resistor (source) for small currents. The system may be viewed as an oscillator with a nonlinear damping coefficient $\gamma(x) = \mu(x^2 - 1)$. By design, for $|x| > 1$, $\gamma > 0$ and the motion is damped while for $|x| < 1$, $\gamma < 0$ and we have 'anti-damping'. As a first order system, we have

$$\dot{x} = p/m, \quad \text{and} \quad \dot{p} = -kx - \frac{\mu}{m}(x^2 - 1)p. \tag{83}$$

The only fixed point is at the origin $(x, p) = (0, 0)$. Linearization around it gives the Jacobian $J = (0, 1/m| - k, \mu/m)$ with $\Delta = k/m > 0$ and $\tau = \mu/m > 0$. So the origin is a spiral source if $\mu^2 < 4km$ and an unstable node if $\mu^2 > 4km$. Either way, trajectories move outward from the origin. On the other hand, for large x and p, the nonlinearity dominates and we have $\dot{p} \approx -(\mu/m)x^2 p$ and $\dot{x} = p/m$, indicating decay of p with x remaining bounded. Thus, due to the balancing effects of damping and anti-damping, we may expect the vdP equation to display a stable limit cycle. With somewhat more effort, it can be shown that the van der Pol equation has a unique stable limit cycle (see Fig. 10). One can find its shape numerically, it is not circular/elliptical (except when $\mu \to 0$) and there is no closed-form expression available for it.

Eg. 3: Brusselator. The Brusselator is a model for an autocatalytic chemical reaction introduced by Ilya Prigogine and collaborators in Brussels. The name is made by combining the words 'Brussels' and 'oscillator'. The Brusselator is described by the pair of differential equations

$$\dot{x} = a - (1 + b)x + x^2 y \quad \text{and} \quad \dot{y} = bx - x^2 y. \tag{84}$$

Check that for $a \neq 0$, it has a unique fixed point at $(x_* = a, y_* = b/a)$. The Jacobian for the linearization around this fixed point is

$$J = \begin{pmatrix} b - 1 & a^2 \\ -b & -a^2 \end{pmatrix} \quad \text{with} \quad \tau = b - 1 - a^2 \quad \text{and} \quad \Delta = a^2. \tag{85}$$

Thus, the fixed point is linearly unstable if $b > 1 + a^2$. A limit cycle forms around this unstable fixed point (see Fig. 11) leading to characteristic oscillations with amplitude independent of initial conditions.

6.5.1 Criteria for non-existence of limit cycles

If we suspect that a system does not admit limit cycles, then it may be possible to rule them out.

Fixed point criterion: From index theory, we have learned that a closed trajectory has index $+1$ and must enclose at least one fixed point. This clearly places a constraint on the occurrence and location of limit cycles. For instance, a limit cycle cannot encircle just two nodes.

Gradient flows do not admit limit cycles: Consider a gradient flow $\dot{\mathbf{r}} = \mathbf{v} = -\nabla W$ in a planar region with W a single-valued scalar 'potential' function. Suppose $\mathbf{r}(t)$ for $t \in [0, T]$ is a closed trajectory (that is not a ring of fixed points). The change in W as we go once round the closed trajectory

$$\Delta W = \int_0^T \frac{dW}{dt}\, dt = \int_0^T \nabla W \cdot \dot{\mathbf{r}}\, dt = -\int_0^T |\nabla W|^2 dt \tag{86}$$

is strictly negative. On the other hand, ΔW must vanish, since W is single-valued. Thus we arrive at a contradiction: we cannot have periodic trajectories in a gradient flow.

Lyapunov Functions: Even if a vector field is not a gradient vector field, we can still rule out closed orbits if it admits a 'Lyapunov' function on phase space that decreases along the flow. More precisely, the C^1 real-valued function $L(\mathbf{r})$ is said to be a Lyapunov function for the flow $\dot{\mathbf{r}} = \mathbf{v}(\mathbf{r})$ if (a) L is positive on the phase space (b) L vanishes only at fixed points and (c) $\dot{L}(\mathbf{r}) < 0$ along the flow as long as $\mathbf{r}$ is not a fixed point. The same argument that we used for gradient flows shows that the existence of a Lyapunov function forbids closed trajectories.

Bendixon's and Dulac's criteria: For a closed trajectory to exist, heuristically, the vector field must go 'round'. On the other hand, if the vector field is 'spreading out' (diverging, $\nabla \cdot \mathbf{v} > 0$) or converging, as in the vicinity of a node, then we cannot have a closed orbit there. This is called Bendixon's criterion. A slight generalization is called Dulac's criterion, which we now describe. Suppose Ω is a simply-connected region in the plane and there exists a smooth function $f(\mathbf{r})$ such that $\nabla \cdot (f(\mathbf{r})\mathbf{v})$ is either strictly positive or strictly negative, then $\mathbf{v}$ cannot have any closed orbits in Ω. The proof uses Green's theorem, which is a planar analogue of Gauss'/Stokes' theorem. Indeed, suppose there is a closed trajectory γ lying inside Ω, then Green's theorem applied to the vector field $f\mathbf{v}$ says that

$$\oint_{\gamma=\partial G} f\mathbf{v} \cdot \hat{n}\, dl = \iint_G \nabla \cdot (f\mathbf{v})\, dxdy \tag{87}$$

where $\hat{n}$ is the outward pointing unit normal on γ, dl is a line element on it and G is the region whose boundary is γ. Since γ is a trajectory, $\mathbf{v}$ must be tangent to it, so $\mathbf{v} \cdot \hat{n} = 0$ and the LHS vanishes. However, by assumption, the RHS is either strictly positive or negative leading to a contradiction. Bendixon's criterion is the special case where $f = 1$. It says that a vector field with $\nabla \cdot \mathbf{v} \neq 0$ in a simply-connected region cannot have any closed orbits contained in that region.

• E.g. We may use Dulac's criterion to rule out closed orbits in the competitive Lotka-Volterra model

$$\dot{r} = r(3 - r - 2s) \quad \text{and} \quad \dot{s} = s(2 - s - r) \quad \text{for} \quad r, s > 1. \tag{88}$$

It is easily checked that this vector field has a divergence that can have either sign in the first quadrant $r, s > 0$. However, suppose we pick $f = 1/rs$, then

$$\nabla \cdot (f\mathbf{v}) = \partial_r \left(\frac{3 - r - 2s}{s} \right) + \partial_s \left(\frac{2 - s - r}{r} \right) = -\left(\frac{1}{r} + \frac{1}{s} \right) < 0. \tag{89}$$

Thus, by Dulac's criterion, the model does not admit any periodic solutions with a positive number of sheep and rabbits.

6.5.2 Poincaré-Bendixon Theorem

The celebrated Poincaré-Bendixon theorem gives sufficient conditions for the existence of a closed orbit in 2d and also places restrictions on what a trajectory can do. In particular, it precludes chaos in 2d autonomous systems. The statement is as follows.

Poincaré-Bendixon Theorem: Suppose the C^1 vector field $\dot{\mathbf{r}} = \mathbf{v}(\mathbf{r})$ is defined in an open subset D of the phase plane and let $K \subset D$ be a compact (closed and bounded) subset that contains no fixed points. Moreover, suppose γ is a 'trapped' trajectory that begins in K (at some time) and remains in K at all subsequent times. Then γ is either a closed orbit or approaches (spirals towards) a closed orbit as $t \to \infty$. Since K contains all its limit points, the limiting closed orbit in the latter case must lie within K. Either way, K contains a closed trajectory.

• From index theory, we know that a closed orbit must enclose a fixed point. Since the theorem requires that K be fixed-point free, K must be chosen to exclude the fixed points that lie within the closed orbit that the theorem guarantees. Thus, in applications of the Poincaré-Bendixon theorem, K is typically chosen to be shaped like an annulus. In practice it may be tricky to identify a trajectory that remains in K. A way to ensure this is to pick K to be a *trapping region*: a connected compact subset of D on whose boundary the vector field points inward. All trajectories that begin in a trapping region are then confined to it. If a trapping region does not contain any fixed points, then the Poincaré-Bendixon theorem guarantees that it has a closed trajectory.

• By a careful choice of a trapping region, one can use the Poincaré-Bendixon theorem to show that the van der Pol oscillator has a closed trajectory.

• **Example:** Apply the Poincaré-Bendixon theorem to show that the vector field

$$\dot{r} = r(1 - r) + \alpha r \sin\theta \quad \text{and} \quad \dot{\theta} = 1 \tag{90}$$

admits a closed trajectory for any sufficiently small $\alpha > 0$.

ANS: We may choose the trapping region to be the annulus $r_{\min} = 1 - \alpha \le r \le r_{\max} = 1 + \alpha$ for any $\alpha < 1$. We need to ensure that $\dot{r} = r(1 - r) + \alpha r \sin\theta > 0$ for $r = r_{\min}$ and $\dot{r} < 0$ for $r = r_{\max}$. Use the fact that $-1 \le \sin\theta \le 1$ to check that this is satisfied.

• **Absence of chaos on the phase plane.** The Poincaré-Bendixon theorem restricts the possible behavior of trajectories on the phase plane. If a trajectory is confined to a compact region without fixed points, the trajectory must either be periodic or approach a periodic orbit. In other words, the trajectory cannot wander around endlessly in a bounded region without

approaching a fixed point or a limit cycle. In both these cases, there is no sensitivity to initial conditions, which is a hallmark of chaos[12].

In three and higher dimensions, phase trajectories confined to a bounded region can be chaotic: they can wander around endlessly without approaching a fixed point or a periodic orbit and display extreme sensitivity to initial conditions. In addition to fixed points, periodic orbits and limit cycles, one encounters 'strange attractors' that are fractals: this happens for instance in Edward Lorenz's 1963 toy-model for atmospheric convection, which has a 3d phase space. For certain classes of initial conditions, the motion is chaotic/irregular: sensitive to initial conditions, remaining bounded and never settling down to periodic motion.

6.6 Bifurcations in two dimensions

We briefly examine some bifurcations of two-dimensional vector fields. In addition to the change in character of fixed points (as in 1d), here we also have the possibility of limit cycles changing stability or being created/destroyed.

6.6.1 Saddle-node, transcritical and pitchfork bifurcations

The saddle-node, transcritical and pitchfork bifurcations generalize in a straightforward manner to 2 and higher dimensions. The flow in the all directions other than one is passive (attractive or repulsive) and the change in character of the vector field is essentially confined to one direction (say x). Thus, normal forms can be chosen to involve decoupled pairs of differential equations for x and y.

• A **saddle-node bifurcation** is exemplified by the normal form

$$\dot{x} = a - x^2 \quad \text{and} \quad \dot{y} = -y. \tag{91}$$

as the control parameter a is varied, this vector field displays the basic mechanism by which fixed points can be produced or annihilated in pairs. While $y(t) = y(0)e^{-t}$ approaches zero exponentially fast, the dynamics in the x direction is as in §3.1. For $a > 0$, we have a saddle at $(-\sqrt{a}, 0)$ and a stable node at $(\sqrt{a}, 0)$. As a decreases to zero, the saddle and node coalesce at a partly stable-partly unstable fixed point at the origin (whose basin of attraction is the closed right half plane) leaving behind no fixed points when $a < 0$. This explains the name saddle-node bifurcation. However, for $a \lesssim 0$, there is a remnant/ghost of the fixed point around $(0, 0)$. Though the flow is generally downward and leftwards (towards an unstable direction of the erstwhile saddle), trajectories are slowed down as the pass through a bottleneck around the origin.

• **Transcritical bifurcation.** Similarly, the transcritical bifurcation (§3.2) generalizes to 2d. The canonical form is

$$\dot{x} = x(a - x) \quad \text{and} \quad \dot{y} = -y. \tag{92}$$

This vector field has fixed points at $(0, 0)$ and $(a, 0)$. For $a < 0$, the origin is a stable node and $(a, 0)$ is a saddle. As a increases past 0, the fixed point at $(a, 0)$ passes through the origin and

[12] In unbounded regions, nearby trajectories can diverge, but then they may fly off to infinity in a regular fashion, as in the Kepler problem.

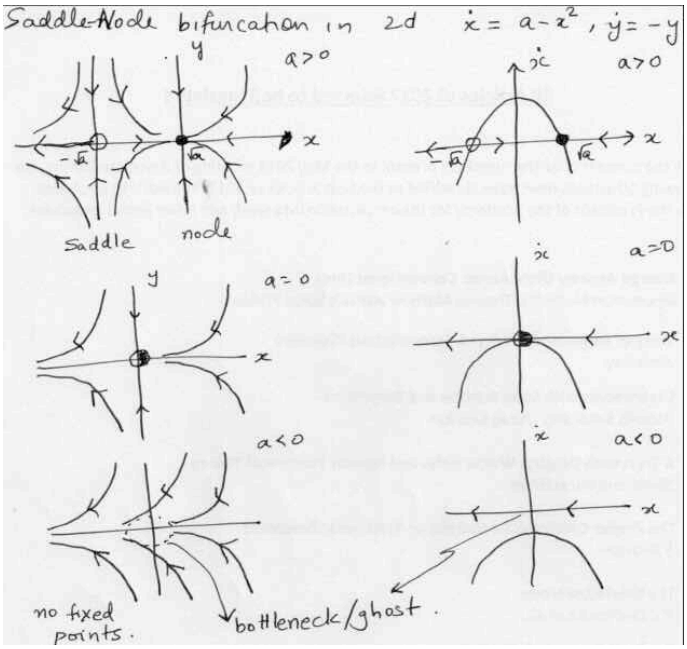

Figure 12: Saddle-Node bifurcation in 2d

exchanges stabilities with it. As a result, for $a > 0$, the origin becomes a saddle while $(a, 0)$ becomes a stable node.

Remark: In all these examples of bifurcations, a stable fixed point has undergone a change in stability as a control parameter is varied. In the linear approximation, the Jacobian of the vector field around a stable fixed point generically has a pair of eigenvalues with negative real parts. These eigenvalues could both be negative (as in the case of a stable node) or be complex conjugates (as in the case of a spiral sink); either way they lie in the left half of the complex eigenvalue plane. The bifurcation is associated with a change in stability, this typically happens when one or both eigenvalues reach the imaginary axis or cross over to the right half-plane. In the above examples, we were dealing with real eigenvalues since nodes and saddles were involved and one of the eigenvalues reached $\lambda = 0$ at the bifurcation point. Thus, they are called zero-eigenvalue bifurcations. The other possibility where a pair of complex conjugate eigenvalues in the left half plane together cross the imaginary axis is qualitatively different and leads to Hopf bifurcations which we turn to next.

6.6.2 Hopf bifurcations

Unlike the saddle-node, transcritical and pitchfork bifurcations which involve collisions between fixed points, Hopf bifurcations do not. A Hopf bifurcation is one way in which a limit cycle can be created or destroyed. Though Hopf bifurcations are not direct generalizations of 1d bifurcations, they bear some resemblance to pitchfork bifurcations and can occur for systems with a state space of dimension two or more.

Supercritical Hopf bifurcation: A supercritical Hopf bifurcation is somewhat analogous to a supercritical pitchfork bifurcation. Thus, we have a stable fixed point $\mathbf{r}_*$ when the control

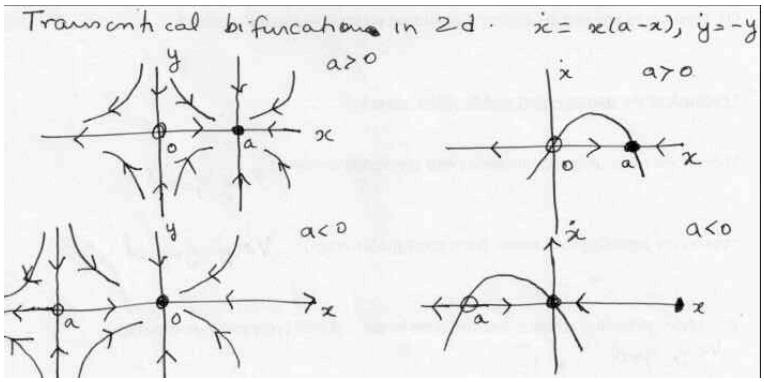

Figure 13: Transcritical bifurcation in 2d

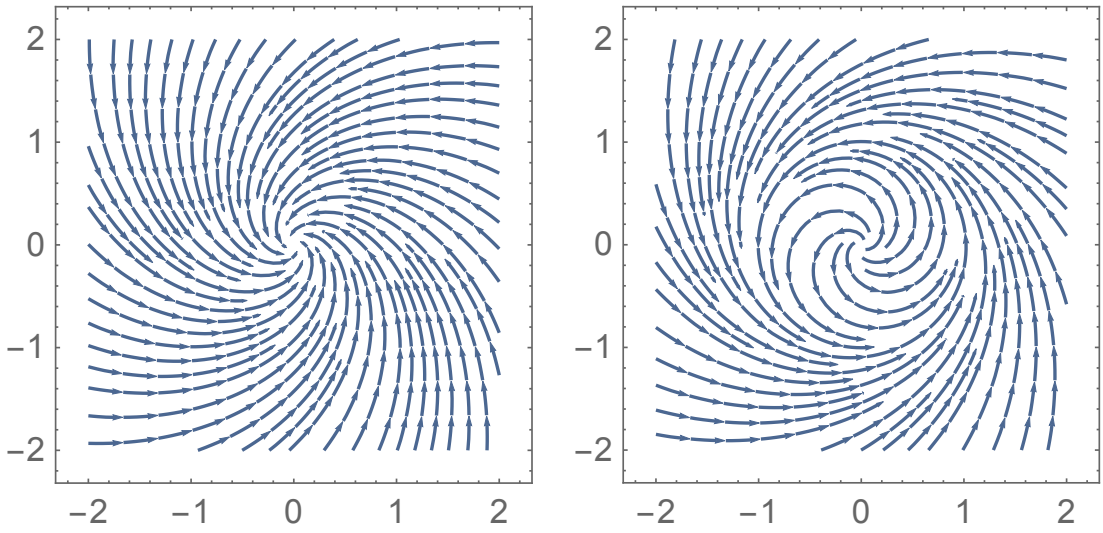

Figure 14: Supercritical Hopf bifurcation of (93). Stable spiral for $a = -1 < 0$ transitions to a stable limit cycle for $a = 1 > 0$. Here $b = \omega = 1$.

parameter is on one side of a critical value, say $a < a_c$. However, rather than being a stable node, it is a spiral sink. Thus, for $a < a_c$ the system displays damped oscillations before settling down to the fixed point. On the other hand, for $a > a_c$, the fixed point becomes a spiral source. However, stability is not entirely lost, since the spiral approaches a stable limit cycle of roughly elliptical shape that encircles $\mathbf{r}_*$. What this means in practice is that the exponential decay to an equilibrium state becomes slower as $a \to a_c^-$. Beyond a_c, the equilibrium state becomes unstable and the system flutters/oscillates about it with relatively small amplitude. One says that the supercritical Hopf bifurcation is safe or soft. A prototypical vector field displaying a supercritical Hopf bifurcation is given by the following system in plane polar coordinates

$$\dot{r} = ar - r^3 \quad \text{and} \quad \dot{\theta} = \omega + br^2 \tag{93}$$

For $a \leq 0$, $\mathbf{r}_* = 0$ is a stable spiral. The approach to the origin goes from exponentially fast to a power law as $a \to 0^-$. When $a > 0$, the origin is a spiral source. However, the unstable spiral

growth saturates (due to the stabilizing effect of the $-r^3$ term) at a stable limit cycle given by the circle $r = \sqrt{a}$ on which $\dot{r} = 0$ and $\dot{\theta} = \omega + ab$. The behavior of eigenvalues of the Jacobian is most easily examined in Cartesian coordinates $x = r\cos\theta$ and $y = r\sin\theta$ where

$$\begin{aligned} \dot{x} &= \cos\theta\,\dot{r} - r\sin\theta\,\dot{\theta} = x(a - r^2) - y(\omega + br^2) = ax - \omega y + \mathcal{O}(x^3, y^3, \cdots) \quad \text{and} \\ \dot{y} &= \sin\theta\,\dot{r} + r\cos\theta\,\dot{\theta} = y(a - r^2) + x(\omega + br^2) = \omega x + ay + \mathcal{O}(x^3, y^3, \cdots). \end{aligned} \tag{94}$$

Thus the linearization around the fixed point at the origin is given by

$$J = \begin{pmatrix} a & -\omega \\ \omega & a \end{pmatrix} \tag{95}$$

with the eigenvalues $\lambda = a \pm i\omega$. Evidently, the eigenvalues cross the imaginary axis from the left to right half plane as a increases past zero.

Subcritical Hopf bifurcations: are dangerous since after the bifurcation, stable oscillations are rendered unstable and trajectories jump to some 'far-away' attractor (a fixed point, a limit cycle, infinity or even a chaotic attractor, as in the case of the Lorenz model). This is illustrated by the vector field

$$\dot{r} = ar + r^3 - r^5 \quad \text{and} \quad \dot{\theta} = \omega + br^2. \tag{96}$$

The linearization around the fixed point at the origin,

$$\begin{aligned} \dot{x} &= \frac{x}{r}\dot{r} - y\dot{\theta} = x(a + r^2 - r^4) - y(\omega + br^2) \approx ax - \omega y \quad \text{and} \\ \dot{y} &= \frac{y}{r}\dot{r} + x\dot{\theta} = y(a + r^2 - r^4) + x(\omega + br^2) \approx \omega x + ay, \end{aligned} \tag{97}$$

leads to the same Jacobian $J = \begin{pmatrix} a & -\omega \\ \omega & a \end{pmatrix}$ as in the above supercritical example. As before, as a increases past 0, the eigenvalues $a \pm i\omega$ cross over to the right half plane making the origin an unstable fixed point. What makes this example different is that the r^3 term in (96) is now destabilizing. As in the subcritical pitchfork example of §3.3.2, this is balanced by a stabilizing r^5 term. The latter will be seen to lead to a large amplitude limit cycle to which trajectories can flow after the bifurcation.

Indeed, for $-1/4 < a < 0$, there is a spiral sink at the origin surrounded by an unstable limit cycle at $r^2 = (1 - \sqrt{1 + 4a})/2$ which is in turn surrounded by a larger stable limit cycle at $r^2 = (1 + \sqrt{1 + 4a})/2$ (see Fig. 15). So for $-1/4 < a < 0$ the system displays decaying oscillations for small amplitude initial conditions. As $a \to 0^-$, the unstable limit cycle shrinks to the origin turning it into an unstable spiral. The decaying oscillations morph into growing oscillations at the subcritical Hopf bifurcation at $a = 0$. In this example, these growing trajectories are then attracted to the far-away limit cycle at $r^2 = (1 + \sqrt{1 + 4a})/2$.

As in the one-dimensional example of §3.3.2, this system displays hysteresis. When a is decreased from positive values, the large amplitude oscillations persist all the way down to $a = -1/4$. At this point, the stable and unstable limit cycles collide and annihilate in a saddle-node bifurcation of cycles and we are left with a spiral sink at the origin for $a < -1/4$.

In addition to Hopf bifurcations, there are other ways in which limit cycles can be created or destroyed in 2d. These are classified as global bifurcations as they involve large regions of the phase plane. (a) We already encountered the **saddle-node or fold bifurcation of cycles** at $a = -1/4$ in the example of (96). Here, a stable and unstable limit cycle that exist for

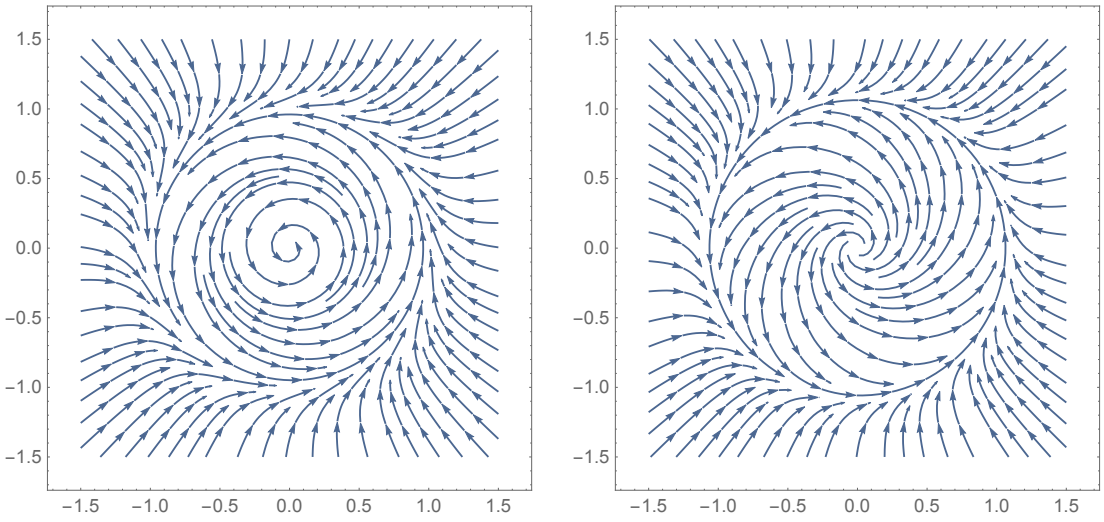

Figure 15: Subcritical Hopf bifurcation of (96) at $a = 0$. Left: stable spiral surrounded by an unstable circular limit cycle and a larger stable limit cycle for $a = -1/5$. Right: Unstable spiral with trajectories attracted to a large amplitude limit cycle for $a = 1/2$. Here $b = \omega = 1$.

$a > -1/4$ annihilate and cease to exist for $a < -1/4$. At $a = -1/4$ they coalesce to form a half-stable cycle. (b) **Saddle-node infinite period bifurcation:** Here, a limit cycle develops a bottleneck and a half-stable fixed point is born on the cycle at the bifurcation point, leading to a divergence of the period. Subsequently, the fixed point splits into a pair of fixed points on the erstwhile cycle in a saddle-node bifurcation. Show that a simple example demonstrating this phenomenon is $\dot{r} = r(1-r^2)$ and $\dot{\theta} = a - \sin\theta$ at $a = 1$. (c) **Homoclinic or saddle-loop bifurcation:** In this case, a limit cycle moves close to a saddle point and touches it when the control parameter reaches its bifurcation point value. As should be plausible from our earlier examples (see §4), this results in a divergence of the period of the limit cycle and the cycle turns into a homoclinic orbit.

7 Lorenz's 3d model of convection and chaos

The Lorenz equations $\dot{\mathbf{r}} = \mathbf{v}(\mathbf{r})$ are a system of three ODEs

$$\dot{x} = \sigma(y - x), \quad \dot{y} = \rho x - y - xz \quad \text{and} \quad \dot{z} = xy - \beta z. \tag{98}$$

They were introduced by Edward Norton Lorenz (J. Atmos. Sci. **20**, 130 (1963)) as a simplified model for atmospheric Rayleigh-Bénard convection cells in a shallow 2d fluid layer warmed from below and cooled from above. He viewed it as a toy system to study the weather and obtained it by reducing a larger system of 12 ODEs used in studying convection. The modes x and y are measures of the velocity and temperature convection rates in the convective roll patterns while z is proportional to the vertical convective heat transfer. The three *positive* parameters ρ, σ and β are constants proportional to the Rayleigh number, Prandtl number (fluid dynamic parameters) and a geometric aspect ratio. Of the three, the Rayleigh number ρ is the main control parameter while σ and β may be taken fixed under typical conditions. In Lorenz's

original work he took $\rho = 28, \sigma = 10$ and $\beta = 8/3$. In addition to convection, the Lorenz equations can also be used to model (geo)dynamos, lasers and water wheels.

• In these variables, the Lorenz equations are quadratically nonlinear and possess the discrete reflection (clockwise-counterclockwise) symmetry $x \to -x, y \to -y$ and $z \to z$.

• If we were to ignore all interaction terms, then the linear system $\dot{x} = -\sigma x$, $\dot{y} = -y$ and $\dot{z} = -bz$ would imply that x, y and z each decays monotonically and exponentially to zero. The full system is much richer.

• **Fixed points:** For $\rho \leq 1$ the trivial fixed point $x_* = y_* = z_* = 0$ is the only fixed point while for $\rho > 1$ two additional nontrivial fixed points emerge. In fact, the conditions for the Lorenz vector field to vanish are

$$\dot{x} = 0 \;\; \Rightarrow \;\; x = y, \quad \dot{y} = 0 \;\; \Rightarrow \;\; x(\rho - 1 - z) = 0 \quad \text{and} \quad \dot{z} = 0 \;\; \Rightarrow \;\; x^2 - \beta z = 0. \tag{99}$$

The second equation implies either $x = 0$ or $z = \rho - 1$. If $x = 0$, then $x_* = y_* = z_* = 0$ is the only possibility. If $z = \rho - 1$ then $x^2 = \beta(\rho - 1)$, which has nontrivial real solutions only if $\rho > 1$. Thus, for $\rho \leq 1$, $\mathbf{r}_* = 0$ is the only fixed point. What is more, for $\rho < 1$, we will use a Lyapunov function to show that $\mathbf{r}_* = 0$ is a global attractor so that the dynamics is relatively benign for $\rho < 1$.

• On the other hand, for $\rho > 1$ we have, in addition to the trivial fixed point, two nontrivial fixed points

$$C_\pm = (x_* = \pm\sqrt{\beta(\rho - 1)},\, y_* = x_*,\, z_* = \rho - 1). \tag{100}$$

Notice that $C_\pm$ merge with the trivial fixed point as $\rho \to 1^+$. The trivial fixed point at the origin corresponds to the absence of convection and no horizontal or vertical temperature variation. The nontrivial fixed points $C_\pm$ correspond to steady clockwise/counter-clockwise convection, which explains the symbol C. As we might expect, the system displays a supercritical pitchfork bifurcation at $\rho = 1$, which is associated with the spontaneous breaking of the above discrete symmetry. It is supercritical since $C_\pm$ are stable for $\rho \gtrsim 1$.

• **Stability of trivial fixed point:** To examine linear stability of fixed points, we consider the Jacobian matrix:

$$J = \left(\frac{\partial v^i}{\partial x^j}\right)_{\mathbf{r}_*} = \begin{pmatrix} -\sigma & \sigma & 0 \\ \rho - z_* & -1 & -x_* \\ y_* & x_* & -\beta \end{pmatrix}. \tag{101}$$

At the trivial fixed point,

$$J(\mathbf{r}_* = 0) = \begin{pmatrix} -\sigma & \sigma & 0 \\ \rho & -1 & 0 \\ 0 & 0 & -\beta \end{pmatrix} \tag{102}$$

and the linearized flow in the z direction decouples and is stable. The restriction of J to the x-y plane is a 2×2 matrix with trace $\tau = -(1 + \sigma) < 0$ (implying stability) and determinant $\Delta = \sigma(1 - \rho)$. Moreover, the discriminant

$$D = \tau^2 - 4\Delta = \sigma^2 + 2\sigma + 1 - 4\sigma + 4\rho\sigma = (\sigma - 1)^2 + 4\rho\sigma > 0 \tag{103}$$

is positive. Thus, if $0 < \rho < 1$, $\Delta > 0$ and the origin is a stable node while if $\rho > 1$, it becomes a saddle point since $\Delta < 0$. This may also be seen from the characteristic equation

$(\lambda+\beta)(\lambda^2+(\sigma+1)\lambda+\sigma(1-\rho))=0$ whose roots are

$$\lambda_\pm = \frac{1}{2}\left(\tau \pm \sqrt{D}\right) \quad \text{and} \quad \lambda_3 = -\beta. \tag{104}$$

• **Contraction of volumes:** The divergence of the vector field $\mathbf{v}$ controls how infinitesimal volumes in the x-y-z phase space change with time. If $(\delta V)(\mathbf{r})$ is an infinitesimal volume located at $\mathbf{r}$,

$$\frac{d}{dt}(\delta V)(\mathbf{r}) = (\nabla\cdot\mathbf{v})(\mathbf{r}) = \text{ tr } J = -(\sigma+1+\beta). \tag{105}$$

Since $\nabla\cdot\mathbf{v}$ is strictly negative and independent of location, little volumes located anywhere in phase space will shrink exponentially in time for any positive σ and β. The system is dissipative in this sense. Thus, any 3d space of initial conditions will eventually shrink (be attracted) to a set of zero volume. This attractor could be one or more fixed points or a limit cycle or invariant surface or some less familiar invariant set of points with zero volume. We will see that the Lorenz system does not admit any invariant surfaces that enclose a finite volume, but that the other possibilities can and do occur for various values of ρ.

• **Origin is a global attractor when $\rho<1$:** Consider the non-negative function

$$\phi = \frac{1}{2}\left(\frac{x^2}{\sigma}+y^2+z^2\right). \tag{106}$$

We will show that for $\rho<1$, ϕ is a Lyapunov function for the Lorenz system. It is clear that ϕ, vanishes only at the trivial fixed point $\mathbf{r}_*=0$ and has concentric ellipses as its level surfaces. It remains to show that ϕ is monotonically decreasing along the flow, so that every trajectory must approach $\mathbf{r}=0$ as $t\to\infty$. To do so, we compute:

$$\begin{aligned}
\dot\phi &= \frac{x\dot x}{\sigma}+y\dot y+z\dot z = (xy-x^2)+(\rho xy-y^2-\cancel{xyz})+(\cancel{xyz}-\beta z^2)\\
&= -(x^2-(\rho+1)xy+y^2+\beta z^2)\\
&= -\left[\left(x-\left(\frac{\rho+1}{2}\right)y\right)^2+\left(1-\left(\frac{\rho+1}{2}\right)^2\right)y^2+\beta z^2\right],
\end{aligned} \tag{107}$$

where we have completed a square. Now for $\rho<1$, $\rho+1<2$ so that $((\rho+1)/2)^2<1$, Thus, for $\rho<1$, $\dot\phi$ is the negative of the sum of three squares with positive coefficients. It follows that $\dot\phi<0$ for $\rho<1$. What is more, we observe that for $\dot\phi$ to vanish, each of the three terms in (107) must vanish. This happens only if $x=y=z=0$, so that ϕ is strictly decreasing along the flow away from the origin. Thus, for $\rho<1$, any trajectory that begins away from $\mathbf{r}=0$ must approach the trivial fixed point as $t\to\infty$. This implies that for $\rho<1$, there cannot be any limit cycles, nontrivial invariant manifolds or chaos.

• What is the nature of the dynamics for $\rho>1$?

• **Stability of nontrivial fixed points $C_\pm$:** The nontrivial fixed points $C_\pm$ (which exist only for $\rho>1$) can be stable or unstable depending on the values of ρ,σ and β. For the values chosen by Lorenz ($\rho=28,\sigma=10$ and $\beta=8/3$), they are unstable: two of the eigenvalues of J have positive real parts: $\lambda_3\approx-13.9, \lambda_\pm\approx 0.09\pm 10.2i$. On the other hand holding σ,β fixed, for a smaller ρ (e.g. $\rho=18$) they are stable $\lambda_3\approx-13.21, \lambda_\pm=-.23\pm 8.3i$. So we might suspect a change in stability of $C_\pm$ at a critical value ρ_H (named since it turns out to be a Hopf

bifurcation) at which $\lambda_\pm$ cross the imaginary axis. To find where this occurs, we note that the Jacobians at $C_\pm$,

$$J(C_\pm) = \begin{pmatrix} -\sigma & \sigma & 0 \\ 1 & -1 & \mp\sqrt{\beta(\rho-1)} \\ \pm\sqrt{\beta(\rho-1)} & \pm\sqrt{\beta(\rho-1)} & -\beta \end{pmatrix}. \tag{108}$$

have the characteristic polynomial

$$\lambda^3 + (1+\beta+\sigma)\lambda^2 + \beta(\rho+\sigma)\lambda + 2\beta\sigma(\rho-1). \tag{109}$$

On the other hand, at the transition, the eigenvalues must be of the form $\lambda = \pm i\omega$ and λ_3 for $\omega, \lambda_3 \in \mathbb{R}$ leading to the characteristic polynomial

$$(\lambda - i\omega)(\lambda + i\omega)(\lambda - \lambda_3) = \lambda^3 - \lambda_3\lambda^2 + \omega^2\lambda - \omega^2\lambda_3. \tag{110}$$

Comparing, we read off $\lambda_3 = -(1+\beta+\sigma)$ [which corresponds to a stable direction], $\omega^2 = \beta(\rho_H + \sigma)$ and $\omega^2\lambda_3 = -2\beta\sigma(\rho_H - 1)$. The latter two equations admit only one solution

$$\rho_H = \sigma\left(\frac{\sigma+\beta+3}{\sigma-\beta-1}\right). \tag{111}$$

Here we assume $\sigma > \beta+1$ so that $\rho_H > 0$ [when $\rho > 1$ and $\sigma < \beta+1$, the nontrivial fixed points $C_\pm$ are unstable]. For the Lorenz values, the inequality is satisfied and $\rho_H = 470/19 \approx 24.7368$, which lies between $\rho = 18$ and $\rho = 28$ we considered above. Thus, $C_\pm$ are linearly stable provided $1 < \rho < \rho_H$.

• **Subcritical Hopf bifurcation:** As $\rho \to \rho_H$ from below, one can show with more effort, that the stable fixed points $C_\pm$ undergo a subcritical Hopf bifurcation. This means that unstable limit cycles shrink to $C_\pm$ as $\rho \to \rho_H^-$ and render the nontrivial fixed points unstable for $\rho > \rho_H$. So for $\rho > \rho_H$, generic trajectories do not approach $C_\pm$ nor the trivial fixed point and do not have the above limit cycles to approach either. What can trajectories do? Can they approach some other limit cycle? Lorenz argued (using a discrete time dynamics 'Lorenz map' concocted from the Lorenz model) that any limit cycles would have to be unstable. Can they approach some invariant surface, such as a torus (and become quasi-periodic)?

• **No invariant surfaces enclosing finite (non-zero) volume in Lorenz system:** We may argue that the Lorenz system cannot have any invariant surfaces that enclose a finite volume (e.g. a closed and bounded surface such as a sphere or a torus or a Riemann surface of higher genus). Indeed, suppose there is such an invariant surface Σ, then the 3d region Ω inside Σ must also be invariant under the flow. In particular, the volume of Ω must be conserved in time. However, this contradicts the previously established (105) exponential decrease in volume of any region of the phase space.

• **Trajectories cannot escape to infinity.** Can trajectories fly off to infinity? It turns out this too is not possible. This can be shown by finding a trapping surface. For example, consider the ellipsoids E_K defined by the level surfaces $F = K$ of the function

$$F(x,y,z) = \rho x^2 + \sigma y^2 + \sigma(z-2\rho)^2. \tag{112}$$

We will show that if K is chosen sufficiently large, then every trajectory that begins on E_K remains inside it. Given any initial condition, there will then be such a trapping surface containing it, establishing that trajectories cannot escape to infinity.

• To see this, we will show that the vector field points inwards on E_K for K big enough. Now, the outward normal on E_K and the Lorentz vector field are given by

$$\nabla F = (2\rho x, 2\sigma y, 2\sigma(z-2\rho)) \quad \text{and} \quad \mathbf{v} = (\sigma(y-x), \rho x - y - xz, xy - \beta z). \tag{113}$$

For $\mathbf{v}$ to point inwards on E_K we need $\mathbf{v}\cdot\nabla F < 0$. Now,

$$\begin{aligned} \mathbf{v}\cdot\nabla F &= 2\sigma\left[\cancel{\rho xy} - \rho x^2 + \cancel{\rho xy} - y^2 - \cancel{xyz} + \cancel{xyz} - \cancel{2\rho xy} - \beta z^2 + 2\rho\beta z\right] \\ &= -2\sigma\left[\rho x^2 + y^2 + \beta(z-\rho)^2 - \beta\rho^2\right]. \end{aligned} \tag{114}$$

For this to be negative we need

$$\rho x^2 + y^2 + \beta(z-\rho)^2 > \beta\rho^2. \tag{115}$$

Here β and ρ are fixed. This condition says that (x, y, z) must lie outside a certain ellipsoid. Though they have different centers and semi-axes, by choosing K sufficiently big, we may ensure E_K lies outside this ellipsoid thereby ensuring the condition is satisfied. Thus, we have our trapping ellipsoids guaranteeing that trajectories cannot escape to infinity.

• Thus, for $\rho > \rho_H$, trajectories are confined to a large ellipsoid in phase space but are generically not attracted to any fixed point, limit cycle or invariant surface enclosing a nonzero volume. This non-periodic and non-quasi-periodic bounded motion may be shown to display extreme sensitivity to initial conditions (with the associated difficulty in making reliable long-term predictions). The dynamics is said to be chaotic. Due to the shrinking of phase space volume, trajectories must approach an attractor of zero volume, it is called a strange attractor and is a fractal set. A typical trajectory for Lorenz's values of parameters is displayed in Fig. 16. For more on the Lorenz attractor and chaos in the Lorenz system, see the book by Strogatz.

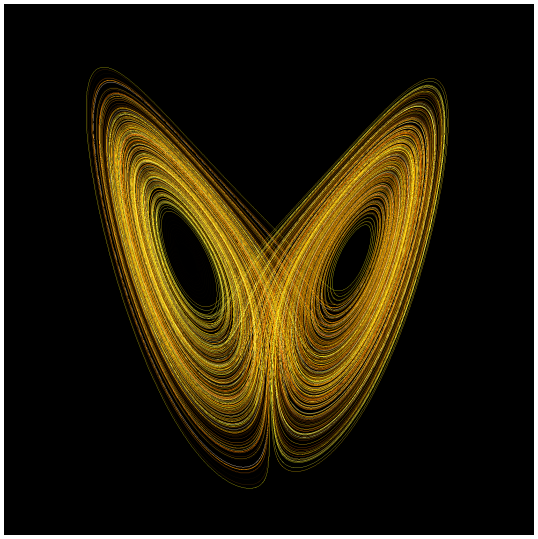

Figure 16: A 'chaotic' trajectory in the Lorenz model (viewed in the x-z plane) for $\rho = 28, \sigma = 10$ and $\beta = 8/3$. The trajectory 'goes round' the 'left lobe' a few times before switching to the right lobe. The lobes are located around the unstable fixed points $C_\pm$. This winding and switching continues indefinitely with no apparent regularity. Figure from Wikipedia.